SAND2019-12937R

Formulation, analysis and computation of an optimization-based local-to-nonlocal coupling method*

Marta D'Elia† *Pavel Bochev*†

Abstract

We present an optimization-based coupling method for local and nonlocal continuum models. Our approach couches the coupling of the models into a control problem where the states are the solutions of the nonlocal and local equations, the objective is to minimize their mismatch on the overlap of the local and nonlocal problem domains, and the virtual controls are the nonlocal volume constraint and the local boundary condition. We present the method in the context of Local-to-Nonlocal diffusion coupling. Numerical examples illustrate the theoretical properties of the approach.

Keywords: Nonlocal diffusion, coupling method, optimization, nonlocal vector calculus.

1 Introduction

Nonlocal continuum theories such as peridynamics [30], physics-based nonlocal elasticity [12], or nonlocal descriptions resulting from homogenization of nonlinear damage models [23] can incorporate strong nonlocal effects due to long-range forces at the mesoscale or microscale. As a result, for problems where these effects cannot be neglected, such descriptions are more accurate than local Partial Differential Equations (PDEs) models. However, their computational cost is also significantly higher than that of PDEs. Local-to-Nonlocal (LtN) coupling methods aim to combine the computational efficiency of PDEs with the accuracy of nonlocal models. The need for LtN couplings is especially acute when the size of the computational domain is such that the nonlocal solution becomes prohibitively expensive to compute, yet the nonlocal model is required to accurately resolve small scale features such as crack tips or dislocations that can affect the global material behavior.

LtN couplings involve two fundamentally different mathematical descriptions of the same physical phenomena. The principal challenge is the stable and accurate merging of these descriptions into a physically consistent coupled formulation. In this paper we address this challenge by couching the LtN coupling into an optimization problem. The objective is to minimize the mismatch of the local and nonlocal solutions on the overlap of their respective subdomains, the constraints are the associated governing equations, and the controls are the virtual nonlocal volume constraint and the local boundary condition. We formulate and analyze this optimization-based LtN approach in the context of local and nonlocal diffusion models [16].

*SNL is a multimission laboratory managed and operated by National Technology and Engineering Solutions of Sandia, LLC., a wholly owned subsidiary of Honeywell International, Inc., for the U.S. Department of Energys National Nuclear Security Administration contract number DE-NA0003525.

†Center for Computing Research, Sandia National Laboratories, Mail Stop 1320 Albuquerque, New Mexico, 87185-1320 ({mdelia,pbboche}@sandia.gov).

Our coupling strategy differs fundamentally from other LtN approaches such as the extension of the Arlequin [11] method to LtN couplings [23], force-based couplings [29], or the morphing approach [5, 25]. The first two schemes blend the energies or the forces of the two models over a dedicated "gluing" area, while the third one implements the coupling through a gradual change in the material properties characterizing the two models over a "morphing" region. In either case, resulting LtN methods treat the coupling condition as a constraint, similar to classical domain decomposition methods. In contrast, we treat this condition as an optimization objective, and keep the two models separate. This strategy brings about valuable theoretical and computational advantages. For instance, the coupled problem passes a patch test by construction and its well-posedness typically follows from the well-posedness of the constraint equations.

Our approach has its roots in non-standard *optimization-based domain decomposition* methods for PDEs [13, 14, 15, 19, 20, 21, 22, 24]. It has also been applied to the coupling of discrete atomistic and continuum models in [27, 28] and multiscale problems [1]. This paper continues the efforts in [8], which presented an initial optimization-based LtN formulation and in [10], which focussed on specializing the formulation to mixed boundary conditions and mixed volume constraints and its practical demonstration using Sandia's agile software components toolkit. The main contributions of this paper include (i) rigorous analysis of the LtN coupling error, (ii) formal proof of the well-posedness of the discretized LtN formulation, and (iii) rigorous convergence analysis.

We have organized the paper as follows. Section 2 introduces notation, basic notions of nonlocal vector calculus and the relevant mathematical models. We present the optimization-based LtN method and prove its well-posedness in Section 3 and study its error in Section 4. Section 5 focusses on the discrete LtN formulation, its well-posedness and numerical analysis. A collection of numerical examples in Section 6 illustrates the theoretical properties of the method using a simple one-dimensional setting.

2 Preliminaries

Let ω be a bounded open domain in $\mathbb{R}^d$, $d = 2, 3$, with Lipschitz-continuous boundary $\partial\omega$. We use the standard notation $H^s(\omega)$ for a Sobolev space of order s with norm and inner product $\|\cdot\|_{s,\omega}$ and $(\cdot,\cdot)_{s,\omega}$, respectively. As usual, $H^0(\omega) := L^2(\omega)$ is the space of all square integrable functions on ω. The subset of all functions in $H^1(\omega)$ that vanish on $\zeta \subset \partial\omega$ is $H^1_\zeta(\omega) := \{u \in H^1(\omega) : \; u|_\zeta = 0\}$.

The nonlocal model in this paper requires nonlocal vector calculus operators [16, §3.2] acting on functions $u(\boldsymbol{x})\colon \mathbb{R}^d \to \mathbb{R}$ and $\boldsymbol{\nu}(\boldsymbol{x},\boldsymbol{y})\colon \mathbb{R}^d \times \mathbb{R}^d \to \mathbb{R}^d$. Let $\gamma(\boldsymbol{x},\boldsymbol{y})\colon \mathbb{R}^d \times \mathbb{R}^d \to \mathbb{R}$ and $\boldsymbol{\alpha}(\boldsymbol{x},\boldsymbol{y})\colon \mathbb{R}^d \times \mathbb{R}^d \to \mathbb{R}^d$ be a non-negative symmetric kernel and an antisymmetric function, respectively, i.e., $\gamma(\boldsymbol{x},\boldsymbol{y}) = \gamma(\boldsymbol{y},\boldsymbol{x}) \geq 0$ and $\boldsymbol{\alpha}(\boldsymbol{y},\boldsymbol{x}) = -\boldsymbol{\alpha}(\boldsymbol{x},\boldsymbol{y})$. The nonlocal *diffusion*[1] of u is an operator $\mathcal{L}(u)\colon \mathbb{R}^d \to \mathbb{R}$ defined by

$$\mathcal{L}u(\boldsymbol{x}) := 2\int_{\mathbb{R}^d} \big(u(\boldsymbol{y}) - u(\boldsymbol{x})\big)\, \gamma(\boldsymbol{x},\boldsymbol{y})\, d\boldsymbol{y} \qquad \boldsymbol{x} \in \mathbb{R}^d,$$

and its nonlocal *gradient* is a mapping $\mathcal{G}(u)\colon \mathbb{R}^d \times \mathbb{R}^d \to \mathbb{R}^d$ given by

$$\mathcal{G}u(\boldsymbol{x},\boldsymbol{y}) := \big(u(\boldsymbol{y}) - u(\boldsymbol{x})\big)\boldsymbol{\alpha}(\boldsymbol{x},\boldsymbol{y}) \qquad \boldsymbol{x},\boldsymbol{y} \in \mathbb{R}^d. \tag{1a}$$

Finally, the nonlocal *divergence* of $\boldsymbol{\nu}(\boldsymbol{x},\boldsymbol{y})$ is a mapping $\mathcal{D}(\boldsymbol{\nu})\colon \mathbb{R}^d \to \mathbb{R}$ defined by[2]

$$\mathcal{D}\boldsymbol{\nu}(\boldsymbol{x}) := \int_{\mathbb{R}^d} \big(\boldsymbol{\nu}(\boldsymbol{x},\boldsymbol{y}) + \boldsymbol{\nu}(\boldsymbol{y},\boldsymbol{x})\big) \cdot \boldsymbol{\alpha}(\boldsymbol{x},\boldsymbol{y})\, d\boldsymbol{y} \qquad \boldsymbol{x} \in \mathbb{R}^d. \tag{1b}$$

[1] More general representations of $\mathcal{L}$, associated with non-symmetric and not necessarily positive kernel functions exist. Such nonlocal operators may define models for non-symmetric diffusion phenomena such as non-symmetric jump processes [9].

[2] The paper [17] shows that the adjoint $\mathcal{D}^* = -\mathcal{G}$.

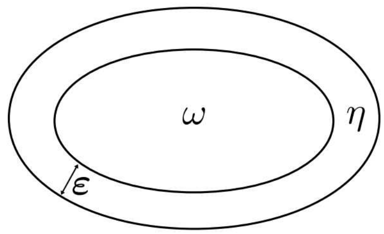

Fig. 1: Two-dimensional domain ω and interaction domain η with interaction radius ε.

Furthermore, given a second-order symmetric tensor $\mathbf{\Phi}(\boldsymbol{x},\boldsymbol{y}) = \mathbf{\Phi}(\boldsymbol{y},\boldsymbol{x})$, equations (1) imply that

$$\mathcal{D}\big(\mathbf{\Phi}\mathcal{G}u\big)(\boldsymbol{x}) = 2\int_{\mathbb{R}^d} \big(u(\boldsymbol{y}) - u(\boldsymbol{x})\big)\big(\boldsymbol{\alpha}(\boldsymbol{x},\boldsymbol{y})\cdot\mathbf{\Phi}(\boldsymbol{x},\boldsymbol{y})\boldsymbol{\alpha}(\boldsymbol{x},\boldsymbol{y})\big)\,d\boldsymbol{y}.$$

Thus, with the identification $\gamma(\boldsymbol{x},\boldsymbol{y}) := \boldsymbol{\alpha}(\boldsymbol{x},\boldsymbol{y})\cdot\mathbf{\Phi}(\boldsymbol{x},\boldsymbol{y})\boldsymbol{\alpha}(\boldsymbol{x},\boldsymbol{y})$ the operator $\mathcal{L}$ is a composition of the nonlocal divergence and gradient operators: $\mathcal{L}u = \mathcal{D}\big(\mathbf{\Phi}\mathcal{G}u\big)$. We define the *interaction domain* of an open bounded region $\omega \in \mathbb{R}^d$ as

$$\eta = \{\boldsymbol{y} \in \mathbb{R}^d \setminus \omega :\ \gamma(\boldsymbol{x},\boldsymbol{y}) \neq 0\},$$

for $\boldsymbol{x} \in \omega$ and set $\Omega = \omega \cup \eta$. In this paper we consider kernels γ such that for $\boldsymbol{x} \in \omega$

$$\begin{cases} \gamma(\boldsymbol{x},\boldsymbol{y}) \geq 0 & \forall\, \boldsymbol{y} \in B_\varepsilon(\boldsymbol{x}) \\ \gamma(\boldsymbol{x},\boldsymbol{y}) = 0 & \forall\, \boldsymbol{y} \in \mathbb{R}^d \setminus B_\varepsilon(\boldsymbol{x}), \end{cases} \tag{2}$$

where $B_\varepsilon(\boldsymbol{x}) = \{\boldsymbol{y} \in \mathbb{R}^d :\ |\boldsymbol{x}-\boldsymbol{y}| \leq \varepsilon\}$. Kernels that satisfy (2) are referred to as localized kernels with *interaction radius* ε. It is easy to see that for such kernels the interaction domain is a layer of thickness ε that surrounds ω, i.e.

$$\eta = \{\boldsymbol{y} \in \mathbb{R}^d \setminus \omega :\ \inf_{\boldsymbol{x}\in\omega} |\boldsymbol{y}-\boldsymbol{x}| \leq \varepsilon\};$$

see Fig. 1 for a two-dimensional example. For a symmetric positive definite tensor $\mathbf{\Phi}$ we respectively define the nonlocal energy semi-norm, nonlocal energy space, and nonlocal volume-constrained energy space by

$$|||v|||^2_\Omega := \frac{1}{2}\int_\Omega\int_\Omega \mathcal{G}v\cdot(\mathbf{\Phi}\mathcal{G}v)\,d\boldsymbol{y}\,d\boldsymbol{x} \tag{3a}$$

$$V(\Omega) := \big\{v \in L^2(\Omega)\ :\ |||v|||_\Omega < \infty\big\} \tag{3b}$$

$$V_\tau(\Omega) := \{v \in V(\Omega)\ :\ v = 0 \text{ on } \tau\}, \quad \text{for } \tau \subseteq \eta. \tag{3c}$$

We also define the volume-trace space $\widetilde{V}(\eta) := \{v|_\eta :\ v \in V(\Omega)\}$, and an associated norm

$$\|\sigma\|_{\widetilde{V}(\eta)} := \inf_{v\in V(\Omega),\, v|_\eta=\sigma} |||v|||_\Omega. \tag{4}$$

We refer to [16, 17] for further information about the nonlocal vector calculus.

In order to avoid technicalities not germane to the coupling scheme, in this paper we consider integrable kernels. Examples of applications modeled by the latter can be found in [2, 3, 4]. Specifically, we assume that there exists positive constants γ_0 and γ_2 such that

$$\gamma_0 \leq \int_{\Omega\cap B_\varepsilon(\boldsymbol{x})} \gamma(\boldsymbol{x},\boldsymbol{y})\,d\boldsymbol{y} \qquad \text{and} \qquad \int_\Omega \gamma(\boldsymbol{x},\boldsymbol{y})^2 d\boldsymbol{y} \leq \gamma_2^2, \tag{5}$$

for all $\boldsymbol{x} \in \Omega$. Note that this also implies that there exists a positive constant γ_1 such that for all $\boldsymbol{x} \in \Omega$

$$\int_\Omega \gamma(\boldsymbol{x}, \boldsymbol{y})\, d\boldsymbol{y} \le \gamma_1. \tag{6}$$

In [16, §4.2] this class of kernels (referred to as Case 2) is rigorously analyzed; we report below an important result, useful throughout the paper.

Lemma 2.1: Let the function γ satisfy (2) and (5), then, there exist positive constants C_{pn} and C^* such that

$$\frac{1}{C_{pn}} \|u\|_{0,\Omega} \le |||u|||_\Omega \le C^* \|u\|_{0,\Omega} \quad \forall\, u \in V_\tau(\Omega). \tag{7}$$

Furthermore, the energy space $V_\tau(\Omega)$ is equivalent to $L^2_\tau(\Omega) = \{v \in L^2(\Omega) : v|_\tau = 0\}$.

The latter is a combination of results in Lemmas 4.6 and 4.7 and Corollary 4.8 in [16, §4.3.2]. Note that the lower bound in (7) represents a nonlocal Poincaré inequality. Even though not included in the analysis, singular kernels appear in applications such as peridynamics; numerical results, included in the paper, suggest that the coupling scheme can handle such kernels without difficulties. However, their analysis is beyond the scope of this paper.

2.1 Local-to-Nonlocal coupling setting

Consider a bounded open region $\omega \subset \mathbb{R}^d$ with interaction domain η. Given $f_n \in L^2(\omega)$ and $\sigma_n \in \widetilde{V}(\eta)$ we assume that the volume-constrained[3] nonlocal diffusion equation

$$\begin{cases} -\mathcal{L}u_n = f_n & \boldsymbol{x} \in \omega \\ u_n = \sigma_n & \boldsymbol{x} \in \eta, \end{cases} \tag{8}$$

provides an accurate description of the relevant physical processes in $\Omega = \omega \cup \eta$. Let $\Gamma = \partial\Omega$, we assume that the local diffusion model given by the Poisson equation

$$\begin{cases} -\Delta u_l = f_l & \boldsymbol{x} \in \Omega \\ u_l = \sigma_l & \boldsymbol{x} \in \Gamma, \end{cases} \tag{9}$$

with suitable boundary data $\sigma_l \in H^{\frac{1}{2}}(\Gamma)$ and forcing term $f_l \in L^2(\Omega)$ is a good approximation of (8) whenever the latter has sufficiently "nice" solutions. In this work we define f_l to be an extension of f_n by 0 in η, specifically,

$$f_l = \begin{cases} f_n & \boldsymbol{x} \in \omega \\ 0 & \boldsymbol{x} \in \eta. \end{cases} \tag{10}$$

For a symmetric positive definite $\boldsymbol{\Phi}$ standard arguments of variational theory show that the weak form[4]

$$\int_\Omega \int_\Omega \mathcal{G}u_n \cdot (\boldsymbol{\Phi}\mathcal{G}z_n)\, d\boldsymbol{y}\, d\boldsymbol{x} = \int_\omega f_n z_n\, d\boldsymbol{x} \qquad \forall\, z_n \in V_\eta(\Omega) \tag{11}$$

[3] The volume constraint in (8) is the nonlocal analogue of a Dirichlet boundary condition.

[4] Multiplication of (8) by a test function $z_n \in V_\eta(\Omega)$, integration over ω and application of the first nonlocal Green's identity [17] yield the weak form (11) of the nonlocal problem.

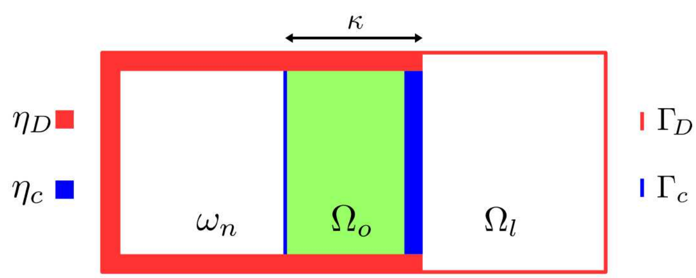

Fig. 2: An example LtN domain configuration in two-dimensions.

of (8) is well-posed [16], i.e., (11) has a unique solution such that

$$|||u_n|||_\Omega \le K_n(\|f_n\|_{0,\omega} + \|\sigma_n\|_{\widetilde{V}(\eta)}) \tag{12}$$

for some positive constant K_n. In this work, for simplicity and without loss of generality, we set $\mathbf{\Phi} = \mathbf{I}$.

Although (11) and the nonlocal calculus [16] enable formulation and analysis of finite elements for (8), which parallel those for the Poisson equation (9), resulting methods may be computationally intractable for large domains. The root cause for this is that long-range interactions increase the density of the resulting algebraic system making it more expensive to assemble and solve.

3 Optimization-based LtN formulation

For clarity we consider (8) and (9) with homogeneous Dirichlet conditions on η and Γ, respectively. To describe the approach it suffices to examine a coupling scenario where these problems operate on two overlapping subdomains of Ω. Thus we consider partitioning of Ω into a nonlocal subdomain ω_n with interaction volume η_n and a local subdomain Ω_l, with boundary Γ_l, such that $\Omega_n := \omega_n \cup \eta_n \subset \Omega$, $\Omega = \Omega_n \cup \Omega_l$ and $\Omega_o = \Omega_n \cap \Omega_l \neq \emptyset$; see Fig. 2. Let $\eta_D = \eta \cap \eta_n$, $\eta_c = \eta_n \setminus \eta_D$, $\Gamma_D = \Gamma \cap \Gamma_l$, and $\Gamma_c = \Gamma_l \setminus \Gamma_D$; see Fig. 2 and Appendix B for a summary of notation and definitions. Restrictions of (8) and (9) to ω_n and Ω_l are given by

$$\left\{\begin{array}{rcll} -\mathcal{L}u_n &=& f_n & \boldsymbol{x} \in \omega_n \\ u_n &=& \theta_n & \boldsymbol{x} \in \eta_c \\ u_n &=& 0 & \boldsymbol{x} \in \eta_D \end{array}\right. \quad \text{and} \quad \left\{\begin{array}{rcll} -\Delta u_l &=& f_l & \boldsymbol{x} \in \Omega_l \\ u_l &=& \theta_l & \boldsymbol{x} \in \Gamma_c \\ u_l &=& 0 & \boldsymbol{x} \in \Gamma_D, \end{array}\right. \tag{13}$$

respectively, where $\theta_n \in \Theta_n = \{v_n|_{\eta_c} : v_n \in V_{\eta_D}(\Omega_n)\}$ and $\theta_l \in \Theta_l = \{v_l|_{\Gamma_c} : v_l \in H^1_{\Gamma_D}(\Omega_l)\}$ are an undetermined Dirichlet volume constraint and an undetermined Dirichlet boundary condition, respectively. The following constrained optimization problem

$$\min_{u_n,u_l,\theta_n,\theta_l} J(u_n,u_l) \text{ subject to (13)}, \quad \text{where } J(u_n,u_l) = \frac{1}{2}\|u_n - u_l\|^2_{0,\Omega_o} \tag{14}$$

defines the optimization-based LtN coupling. In this formulation the subdomain problems (13) are the optimization constraints, u_n and u_l are the states and θ_n and θ_l are the controls. We equip the control space $\Theta_n \times \Theta_l$ with the norm

$$\|(\sigma_n,\sigma_l)\|^2_{\Theta_n\times\Theta_l} = \|\sigma_n\|^2_{0,\eta_c} + \|\sigma_l\|^2_{\frac{1}{2},\Gamma_c}. \tag{15}$$

In contrast to blending, (14) is an example of a divide-and-conquer strategy as the local and nonlocal problems operate independently in Ω_n and Ω_l.

Given an optimal solution $(u_n^*, u_l^*, \theta_n^*, \theta_l^*) \in V_{\eta_D}(\Omega_n) \times H^1_{\Gamma_D}(\Omega_l) \times \Theta_n \times \Theta_l$ of (14) we define the LtN solution $u^* \in L^2(\Omega)$ by splicing together the optimal states:

$$u^* = \begin{cases} u_n^* & \boldsymbol{x} \in \Omega_n \\ u_l^* & \boldsymbol{x} \in \Omega_l \setminus \Omega_o. \end{cases} \tag{16}$$

The next section verifies that (14) is well-posed.

3.1 Well-posedeness

We show that for any pair of controls subproblems (13) have unique solutions $u_n(\theta_n)$ and $u_l(\theta_l)$, respectively. Elimination of the states from (14) yields the equivalent reduced space form of this problem in terms of θ_n and θ_l only:

$$\min_{\theta_n,\theta_l} J(\theta_n, \theta_l) \quad \text{where} \quad J(\theta_n, \theta_l) = \frac{1}{2}\|u_n(\theta_n) - u_l(\theta_l)\|^2_{0,\Omega_o}. \tag{17}$$

To show that (17) is well-posed we start as in [19, 27] and split, for any given (θ_n, θ_l), the solutions of the state equations into a harmonic and a homogeneous part. The harmonic components $v_n(\theta_n)$ and $v_l(\theta_l)$ of the states solve the equations

$$\begin{cases} -\mathcal{L}v_n &= 0 & \boldsymbol{x} \in \omega_n \\ v_n &= \theta_n & \boldsymbol{x} \in \eta_c \\ v_n &= 0 & \boldsymbol{x} \in \eta_D, \end{cases} \quad \text{and} \quad \begin{cases} -\Delta v_l &= 0 & \boldsymbol{x} \in \Omega_l \\ v_l &= \theta_l & \boldsymbol{x} \in \Gamma_c \\ v_l &= 0 & \boldsymbol{x} \in \Gamma_D, \end{cases} \tag{18}$$

respectively. The homogeneous components u_n^0 and u_l^0 solve a similar set of equations but with homogeneous volume constraint and boundary condition, respectively:

$$\begin{cases} -\mathcal{L}u_n^0 &= f_n & \boldsymbol{x} \in \omega_n \\ u_n^0 &= 0 & \boldsymbol{x} \in \eta_n \end{cases} \quad \text{and} \quad \begin{cases} -\Delta u_l^0 &= f_l & \boldsymbol{x} \in \Omega_l \\ u_l^0 &= 0 & \boldsymbol{x} \in \Gamma_l. \end{cases} \tag{19}$$

In terms of these components $u_n = v_n(\theta_n) + u_n^0$, $u_l = v_l(\theta_l) + u_l^0$, and the objective

$$J(\theta_n, \theta_l) = \frac{1}{2}\|v_n(\theta_n) - v_l(\theta_l)\|^2_{0,\Omega_o} + \big(u_n^0 - u_l^0, v_n(\theta_n) - v_l(\theta_l)\big)_{0,\Omega_o} + \frac{1}{2}\|u_n^0 - u_l^0\|^2_{0,\Omega_o}.$$

The Euler-Lagrange equation of (17) is given by: seek $(\sigma_n, \sigma_l) \in \Theta_n \times \Theta_l$ such that

$$Q(\sigma_n, \sigma_l; \mu_n, \mu_l) = F(\mu_n, \mu_l) \quad \forall\, (\mu_n, \mu_l) \in \Theta_n \times \Theta_l, \tag{20}$$

where $Q(\sigma_n, \sigma_l; \mu_n, \mu_l) = \big(v_n(\sigma_n) - v_l(\sigma_l),\, v_n(\mu_n) - v_l(\mu_l)\big)_{0,\Omega_o}$ and $F(\mu_n, \mu_l) = -\big(u_n^0 - u_l^0, v_n(\mu_n) - v_l(\mu_l)\big)_{0,\Omega_o}$. The following lemma establishes a key property of Q.

Lemma 3.1: The form $Q(\cdot;\cdot)$ defines an inner product on $\Theta_n \times \Theta_l$.

Proof. By construction $Q(\cdot;\cdot)$ is symmetric and bilinear. Thus, it suffices to show that $Q(\cdot;\cdot)$ is positive definite, i.e., $Q(\sigma_n, \sigma_l; \sigma_n, \sigma_l) = 0$ if and only if $(\sigma_n, \sigma_l) = (0, 0)$. Let $(\sigma_n, \sigma_l) = (0, 0)$ then $v_n(\sigma_n) = 0$ and $v_l(\sigma_l) = 0$, implying $Q(\sigma_n, \sigma_l; \sigma_n, \sigma_l) = 0$. Conversely, if $Q(\sigma_n, \sigma_l; \sigma_n, \sigma_l) = 0$, then $v_n(\sigma_n) - v_l(\sigma_l) = 0$ in Ω_o. Let $v = v_n(\sigma_n) = v_l(\sigma_l)$ in Ω_o. Then we have that (i) $\Delta v = 0$ for all $\boldsymbol{x} \in \Omega_o$, i.e., v is harmonic in Ω_o, and (ii) $v = 0$ for all $\boldsymbol{x} \in \Omega_o \cap \eta_D$, i.e., v vanishes on a non-empty interior set of Ω_o. By the identity principle for harmonic functions, $v \equiv 0$ in $\overline{\Omega_o}$. Because $\sigma_n = v$ in η_c and $\sigma_l = v$ on Γ_c it follows that $(\sigma_n, \sigma_l) = (0, 0)$. □

As a results, $Q(\cdot;\cdot)$ endows the control space $\Theta_n \times \Theta_l$ with the "energy" norm

$$\|(\sigma_n, \sigma_l)\|_*^2 := Q(\sigma_n, \sigma_l; \sigma_n, \sigma_l) = \|v_n(\sigma_n) - v_l(\sigma_l)\|_{0,\Omega_o}^2. \tag{21}$$

Note that Q and F are continuous with respect to the energy norm. However, the control space $\Theta_n \times \Theta_l$ may not be complete with respect to the energy norm. In this case, following [1, 13], we consider the optimization problem (17) on the completion $\widetilde{\Theta}_n \times \widetilde{\Theta}_l$ of the control space.

Theorem 3.1: Let $\widetilde{\Theta}_n \times \widetilde{\Theta}_l$ denote a completion[5] of the control space with respect to the energy norm (21). Then, the minimization problem

$$\min_{(\theta_n, \theta_l) \in \widetilde{\Theta}_n \times \widetilde{\Theta}_l} J(\theta_n, \theta_l) \tag{22}$$

has a unique minimizer $(\widetilde{\theta}_n^*, \widetilde{\theta}_l^*) \in \widetilde{\Theta}_n \times \widetilde{\Theta}_l$ such that

$$\widetilde{Q}(\widetilde{\theta}_n^*, \widetilde{\theta}_l^*; \mu_n, \mu_l) = \widetilde{F}(\mu_n, \mu_l) \quad \forall\, (\mu_n, \mu_l) \in \widetilde{\Theta}_n \times \widetilde{\Theta}_l. \tag{23}$$

Proof. Equation (23) is a necessary condition for any minimizer of (22). Assume first that the control space is complete, i.e. $\Theta_n \times \Theta_l = \widetilde{\Theta}_n \times \widetilde{\Theta}_l$. Then $\Theta_n \times \Theta_l$ is Hilbert and the projection theorem implies that (23) has a unique solution.

When $\Theta_n \times \Theta_l$ is not complete, the continuous bilinear form Q and the continuous functional F defined on $\Theta_n \times \Theta_l$ can be uniquely extended by using the Hahn-Banach theorem to a continuous bilinear form $\widetilde{Q}$ and a continuous functional $\widetilde{F}$ in $\widetilde{\Theta}_n \times \widetilde{\Theta}_l$. Then, the existence and uniqueness of the minimizer follow as before. □

To avoid technical distractions, in what follows we assume that the minimizer (θ_n^*, θ_l^*) belongs to $\Theta_n \times \Theta_l$ and hence $u_n^* = u_n(\theta_n^*) \in V_{\eta_D}(\Omega_n)$ and $u_l^* = u_l(\theta_l^*) \in H^1_{\Gamma_D}(\Omega_l)$. We note that in the finite dimensional case the completeness is not an issue, as the discrete control space is Hilbert with respect to the discrete energy norm, see Section 5.

4 Analysis of the LtN coupling error

We define the LtN coupling error as the L^2-norm of the difference between the global nonlocal solution $\widehat{u}_n$ of (8) with homogeneous volume constraints and the LtN solution $u^* \in L^2(\Omega)$ given by (16). This section shows that the coupling error is bounded by the *modeling error* on the local subdomain, i.e., the error made by replacing the "true" nonlocal diffusion operator on Ω_l by the Laplacian.

We prove this result under the following assumptions.

H.1 The kernel γ satisfies (2) and (5).

H.2 The global nonlocal solution[6] $\widehat{u}_n \in H^1(\Omega)$.

We also need the *trace* operator $T : H^1(\Omega) \to \Theta_n \times \Theta_l$ such that

$$T(v) := (T_n(v),\ T_l(v)) = (v|_{\eta_c},\ v|_{\Gamma_c}) \qquad \forall\, v \in H^1(\Omega), \tag{24}$$

[5] If $\Theta_n \times \Theta_l$ is complete, then of course we have that $\widetilde{\Theta}_n \times \widetilde{\Theta}_l = \Theta_n \times \Theta_l$.

[6] This assumption can be relaxed to: $\widehat{u}_n \in L^2(\Omega)$ has a well-defined trace on Γ_c.

and the lifting operator $L : \Theta_n \times \Theta_l \to L^2(\Omega)$, $L(\sigma_n, \sigma_l) = H(\sigma_n, \sigma_l) + u^0$, where

$$H(\sigma_n, \sigma_l) := \begin{cases} v_n(\sigma_n) & \Omega_n \\ v_l(\sigma_l) & \Omega_l \setminus \Omega_o, \end{cases} \qquad \text{and} \qquad u^0 := \begin{cases} u_n^0 & \Omega_n \\ u_l^0 & \Omega_l \setminus \Omega_o \end{cases} \tag{25}$$

are a harmonic lifting operator and the homogenous part of the states, respectively. Our main result is the following theorem.

Theorem 4.1: Assume that H.1 and H.2 hold. Then, there exists a positive constant C such that

$$\|\widehat{u}_n - u^*\|_{0,\Omega} \le C \|\widehat{u}_n - \widehat{u}_l\|_{0,\Omega_l} ,$$

where $\widehat{u}_l = v_l(T_l(\widehat{u}_n)) + u_l^0$.

For clarity we break the proof into several steps.

4.1 The harmonic lifting operator is bounded from above

We prove that H is bounded in the operator norm $\|\cdot\|_{**}$ induced by the energy norm (21). We refer to Appendix A for additional notation and auxiliary results used in the proof. We introduce the space $\widetilde{V}_\tau(\eta) = \{\mu \in \widetilde{V}(\eta) : \mu|_\tau = 0, \text{ for } \tau \subseteq \eta\}$.

Lemma 4.1: Assume that H.1 holds. There exists a positive constant $C < \infty$ such that

$$\|H\|_{**} = \sup_{(0,0) \neq (\sigma_n, \sigma_l) \in \Theta_n \times \Theta_l} \frac{\|H(\sigma_n, \sigma_l)\|_{0,\Omega}}{\|(\sigma_n, \sigma_l)\|_*} < \frac{C}{\kappa}, \tag{26}$$

where κ is the thickness of Ω_o.

Proof. To prove (26) it suffices to show that

$$\|H(\sigma_n, \sigma_l)\|_{0,\Omega} \le \widetilde{C} \|(\sigma_n, \sigma_l)\|_* \qquad \forall (0,0) \neq (\sigma_n, \sigma_l) \in \Theta_n \times \Theta_l,$$

For some positive constant $\widetilde{C}$, inversely proportional to κ. According to the definitions of H and $\|(\cdot,\cdot)\|_*$ in (25) and (21), this is equivalent to

$$\|\chi(\Omega_n) v_n(\sigma_n) + \chi(\Omega_l \setminus \Omega_o) v_l(\sigma_l)\|_{0,\Omega} \le \widetilde{C} \|v_n(\sigma_n) - v_l(\sigma_l)\|_{0,\Omega_o},$$

where $\chi(\cdot)$ is the indicator function. Since $(\Omega_l \setminus \Omega_o) \cap \Omega_n = \emptyset$, this inequality reduces to

$$\|v_n(\sigma_n)\|^2_{0,\Omega_n} + \|v_l(\sigma_l)\|^2_{0,\Omega_l \setminus \Omega_o} \le \widetilde{C}^2 \|v_n(\sigma_n) - v_l(\sigma_l)\|^2_{0,\Omega_o}.$$

The strong Cauchy-Schwarz inequality for the harmonic component (see Lemma A.3) yields the following lower bound for the right hand side:

$$\begin{aligned} \|v_n(\sigma_n) - v_l(\sigma_l)\|^2_{0,\Omega_o} &= \|v_n(\sigma_n)\|^2_{0,\Omega_o} - 2(v_n(\sigma_n), v_l(\sigma_l))_{0,\Omega_o} + \|v_l(\sigma_l)\|^2_{0,\Omega_o} \\ &\ge \|v_n(\sigma_n)\|^2_{0,\Omega_o} - 2\delta \|v_n(\sigma_n)\|_{0,\Omega_o} \|v_l(\sigma_l)\|_{0,\Omega_o} + \|v_l(\sigma_l)\|^2_{0,\Omega_o} \\ &\ge (1-\delta)\big(\|v_n(\sigma_n)\|^2_{0,\Omega_o} + \|v_l(\sigma_l)\|^2_{0,\Omega_o}\big). \end{aligned} \tag{27}$$

We now proceed to bound $\|v_n(\sigma_n)\|_{0,\Omega_o}$ and $\|v_l(\sigma_l)\|_{0,\Omega_o}$ from below by $\|v_n(\sigma_n)\|_{0,\Omega_n}$ and $\|v_l(\sigma_l)\|_{0,\Omega_l\setminus\Omega_o}$, respectively. We start with the nonlocal term. Let $\mu_n \in \widetilde{V}_{\eta_D}(\eta_n)$ denote the extension of σ_n by zero in η_D, i.e., $\mu_n = \sigma_n$ in η_c and 0 in η_D. By using the nonlocal Poincaré inequality, the well-posedness of the nonlocal problem and Lemma A.2 we have

$$\begin{aligned}
\|v_n(\sigma_n)\|_{0,\Omega_n} &\le C_{pn}|||v_n(\sigma_n)|||_{\Omega_n} && \text{nonlocal Poincaré inequality (7)}\\
&\le C_{pn}K_n\|\mu_n\|_{\widetilde{V}(\eta_n)} && \text{nonlocal well-posedness (12)}\\
&\le C_{pn}K_nK_1\|\mu_n\|_{0,\eta_n} && \text{Lemma A.2}\\
&\le C_{pn}K_nK_1K_2\|v_n(\sigma_n)\|_{0,\Omega_o}.
\end{aligned}$$

Therefore, we have that

$$\|v_n(\sigma_n)\|^2_{0,\Omega_n} \le \widetilde{C}_n\|v_n(\sigma_n)\|^2_{0,\Omega_o}, \tag{28}$$

with $\widetilde{C} = C_{pn}K_nK_1K_2$.

To analyze the local term we derive a Caccioppoli-type inequality for the local harmonic component. We introduce the cutoff function $g \in C^1(\Omega_l)$ such that $g = 1$ in $\overline{\Omega_l \setminus \Omega_o}$, $g = 0$ in $\Omega\setminus\Omega_l$, $\|\nabla g\|_\infty \le \frac{1}{\kappa}$, and $\text{supp}(\nabla g) \subset \Omega_o$, where κ is the thickness of the overlap, see Fig. 2. These properties imply that gv_l and g^2v_l belong to $H^1_0(\Omega_l)$. Next, we note that v_l is the solution of the weak formulation of (9) with $f_l = 0$. Using g^2v_l as a test function then yields the following identity

$$0 = \int_{\Omega_l} \nabla v_l\nabla(g^2v_l)\,d\boldsymbol{x} = 2\int_{\Omega_l} gv_l\,\nabla v_l\nabla g\,d\boldsymbol{x} + \int_{\Omega_l} g^2\nabla v_l\nabla v_l\,d\boldsymbol{x}.$$

We use the latter to find a bound on $\|\nabla(gv_l)\|_{0,\Omega_l}$:

$$\begin{aligned}
\|\nabla(gv_l)\|^2_{0,\Omega_l} &= \int_{\Omega_l}\nabla(gv_l)\nabla(gv_l)\,d\boldsymbol{x} - \int_{\Omega_l}\nabla v_l\nabla(g^2v_l)\,d\boldsymbol{x}\\
&= \int_{\Omega_l}\nabla(gv_l)\nabla(gv_l)\,d\boldsymbol{x} - 2\int_{\Omega_l} gv_l\,\nabla v_l\nabla g\,d\boldsymbol{x} - \int_{\Omega_l} g^2\nabla v_l\nabla v_l\,d\boldsymbol{x}\\
&= \int_{\Omega_l} v_l^2\nabla g\nabla g\,d\boldsymbol{x} = \int_{\Omega_o} v_l^2\nabla g\nabla g\,d\boldsymbol{x} \le \frac{1}{\kappa^2}\int_{\Omega_o} v_l^2\,d\boldsymbol{x} = \frac{1}{\kappa^2}\|v_l\|^2_{0,\Omega_o}.
\end{aligned}$$

Thus, we conclude that

$$\|v_l\|_{0,\Omega_l\setminus\Omega_o} = \|gv_l\|_{0,\Omega_l\setminus\Omega_o} \le \|gv_l\|_{0,\Omega_l} \le C_p\|\nabla(gv_l)\|_{0,\Omega_l} \le \frac{C_p}{\kappa}\|v_l\|_{0,\Omega_o},$$

where C_p is the local Poincaré constant. Let $\widetilde{K}_{nl} = \max\{\widetilde{C}_n, C_p^2\}$. Together with (27) and (28) this yields

$$\begin{aligned}
\|v_n(\sigma_n)\|^2_{0,\Omega_n} + \|v_l(\sigma_l)\|^2_{0,\Omega_l\setminus\Omega_o} &\le \frac{\widetilde{K}^2_{nl}}{\kappa^2}\left(\|v_n(\sigma_n)\|^2_{0,\Omega_o} + \|v_l(\sigma_l)\|^2_{0,\Omega_o}\right)\\
&\le \frac{\widetilde{K}^2_{nl}}{\kappa^2(1-\delta)}\|v_n(\sigma_n) - v_l(\sigma_l)\|^2_{0,\Omega_o}.
\end{aligned}$$

□

4.2 The approximation error is bounded by the modeling error

The optimal solution (θ_n^*, θ_l^*) of the reduced space problem (17) approximates the trace of the global nonlocal solution $\widehat{u}_n$ on η_c and Γ_c, respectively. The following lemma shows that the error in (θ_n^*, θ_l^*) is bounded by the modeling error on Ω_l.

Lemma 4.2: Let $\widehat{u}_n$ and (θ_n^*, θ_l^*) solve (8) and (17), respectively. Then,

$$\|T(\widehat{u}_n) - (\theta_n^*, \theta_l^*)\|_* \le \|\widehat{u}_n - \widehat{u}_l\|_{0,\Omega_o}. \tag{29}$$

Proof. Because (θ_n^*, θ_l^*) satisfies the Euler-Lagrange equation (20) we have

$$Q(\theta_n^*, \theta_l^*; \mu_n, \mu_l) = -\big(u_n^0 - u_l^0, v_n(\mu_n) - v_l(\mu_l)\big)_{0,\Omega_o} \quad \forall\, (\mu_n, \mu_l) \in \Theta_n \times \Theta_l. \tag{30}$$

Using this identity together with the energy norm definition (21) yields

$$\begin{aligned}
Q(T(\widehat{u}_n) - (\theta_n^*, \theta_l^*); \mu_n, \mu_l) &= Q(T(\widehat{u}_n); \mu_n, \mu_l) - Q(\theta_n^*, \theta_l^*; \mu_n, \mu_l) \\
&= \big(v_n(T_n(\widehat{u}_n)) - v_l(T_l(\widehat{u}_n)), v_n(\mu_n) - v_l(\mu_l)\big)_{0,\Omega_o} + \big(u_n^0 - u_l^0, v_n(\mu_n) - v_l(\mu_l)\big)_{0,\Omega_o} \\
&= \big(\widehat{u}_n - \widehat{u}_l, v_n(\mu_n) - v_l(\mu_l)\big)_{0,\Omega_o} \le \|\widehat{u}_n - \widehat{u}_l\|_{0,\Omega_o} \|v_n(\mu_n) - v_l(\mu_l)\|_{0,\Omega_o} \\
&= \|\widehat{u}_n - \widehat{u}_l\|_{0,\Omega_o} \|(\mu_n, \mu_l)\|_*.
\end{aligned}$$

The lemma follows by setting $(\mu_n, \mu_l) = T(\widehat{u}_n) - (\theta_n^*, \theta_l^*)$ above and observing that $Q(T(\widehat{u}_n) - (\theta_n^*, \theta_l^*); T(\widehat{u}_n) - (\theta_n^*, \theta_l^*)) = \|T(\widehat{u}_n) - (\theta_n^*, \theta_l^*)\|_*^2$. □

4.3 Proof of Theorem 4.1

Let $\widehat{u} := L(T(\widehat{u}_n))$. Definitions (24) and (25) together with the identities

$$\widehat{u}_n|_{\Omega_n} = v_n(T_n(\widehat{u}_n)) + u_n^0 \quad \text{and} \quad \widehat{u}_l = v_l(T_l(\widehat{u}_n)) + u_l^0, \tag{31}$$

imply that

$$\widehat{u} = \begin{cases} \widehat{u}_n & \boldsymbol{x} \in \Omega_n \\ \widehat{u}_l & \boldsymbol{x} \in \Omega_l \setminus \Omega_o. \end{cases} \tag{32}$$

Likewise, the identities $u_n^* = v_n(\theta_n^*) + u_n^0$ and $u_l^* = v_l(\theta_l^*) + u_l^0$ imply that $u^* = L(\theta_n^*, \theta_l^*)$. Adding and subtracting $\widehat{u}$ to the LtN error then yields

$$\begin{aligned}
\|\widehat{u}_n - u^*\|_{0,\Omega} &\le \|\widehat{u}_n - \widehat{u}\|_{0,\Omega} + \|\widehat{u} - u^*\|_{0,\Omega} \\
&= \|\widehat{u}_n - L(T(\widehat{u}_n))\|_{0,\Omega} + \|L(T(\widehat{u}_n)) - L(\theta_n^*, \theta_l^*)\|_{0,\Omega} \\
&= \|\widehat{u}_n - L(T(\widehat{u}_n))\|_{0,\Omega} + \|H(T(\widehat{u}_n)) - H(\theta_n^*, \theta_l^*)\|_{0,\Omega}\,.
\end{aligned} \tag{33}$$

The first term in (33) is the *consistency error* of L; (32) implies that

$$\|\widehat{u}_n - L(T(\widehat{u}_n))\|_{0,\Omega} = \|\widehat{u}_n - \widehat{u}_l\|_{0,\Omega_l \setminus \Omega_o}. \tag{34}$$

To estimate the second term we use (26) and (29):

$$\|H(T(\widehat{u}_n)) - H(\theta_n^*, \theta_l^*)\|_{0,\Omega} \le \|H\|_{**} \|T(\widehat{u}_n) - (\theta_n^*, \theta_l^*)\|_* \le \frac{C}{\kappa} \|\widehat{u}_n - \widehat{u}_l\|_{0,\Omega_o}.$$

Combining (33) with this bound and (34) gives

$$\|\widehat{u}_n - u^*\|_{0,\Omega} \le \|\widehat{u}_n - \widehat{u}_l\|_{0,\Omega_l\setminus\Omega_o} + \frac{C}{\kappa}\|\widehat{u}_n - \widehat{u}_l\|_{0,\Omega_o} \le \left(1 + \frac{C}{\kappa}\right)\|\widehat{u}_n - \widehat{u}_l\|_{0,\Omega_l},$$

which completes the proof. □

4.4 Convergence of the modeling error

In this section we show that $\|\widehat{u}_n - \widehat{u}_l\|_{0,\Omega_l}$ vanishes as $\varepsilon \to 0$.

Lemma 4.3: Let $\widehat{u}_n$ be the solution of (8) with homogeneous volume constraints and let $\widehat{u}_l$ be defined as in (31). Assume that H.1 and H.2 hold; then,

$$\lim_{\varepsilon\to 0}\|\widehat{u}_n - \widehat{u}_l\|_{0,\Omega_l} = 0.$$

Proof. By definition $\widehat{u}_l$ solves the boundary value problem

$$\begin{cases} -\Delta\widehat{u}_l &= f_l & \boldsymbol{x}\in\Omega_l \\ \widehat{u}_l &= \widehat{u}_n & \boldsymbol{x}\in\Gamma_c \\ \widehat{u}_l &= 0 & \boldsymbol{x}\in\Gamma_D, \end{cases}$$

and so, it is also a solution of the weak equation

$$\int_{\Omega_l}\nabla\widehat{u}_l\cdot\nabla w d\boldsymbol{x} = \int_{\Omega_l} f_l\, w d\boldsymbol{x} \quad \forall\, w\in H_0^1(\Omega_l).$$

Let $\psi\in H_0^1(\Omega_l)$ solve the dual problem

$$\int_{\Omega_l}\nabla w\cdot\nabla\psi d\boldsymbol{x} = \int_{\Omega_l}(\widehat{u}_l - \widehat{u}_n) w d\boldsymbol{x} \quad \forall\, w\in H_0^1(\Omega_l)\,. \tag{35}$$

Since $\widehat{u}_l - \widehat{u}_n = 0$ on Γ_l one can set $w = \widehat{u}_l - \widehat{u}_n$ in (35) to obtain

$$\begin{aligned} \|\widehat{u}_l - \widehat{u}_n\|^2_{0,\Omega_l} &= \int_{\Omega_l}\nabla(\widehat{u}_l - \widehat{u}_n)\cdot\nabla\psi d\boldsymbol{x} \\ &= \int_{\Omega_l} f_l\psi d\boldsymbol{x} - \int_{\Omega_l}\nabla\widehat{u}_n\cdot\nabla\psi d\boldsymbol{x} \\ &= \int_{\Omega_l\cap\eta} f_l\psi d\boldsymbol{x} + \textstyle\int_{\Omega_l\setminus\eta} f_n\psi d\boldsymbol{x} - \int_{\Omega_l}\nabla\widehat{u}_n\cdot\nabla\psi d\boldsymbol{x} \\ &= \int_{\Omega_l\setminus\eta}\mathcal{L}\widehat{u}_n\psi d\boldsymbol{x} - \int_{\Omega_l\setminus\eta}\nabla\widehat{u}_n\cdot\nabla\psi d\boldsymbol{x} \to 0, \qquad \text{as } \varepsilon\to 0, \end{aligned}$$

where the third equality follows from the fact that f_l is extended to zero in η and the limit follows from the result in [17, Section 5][7]. □

[7] It can be shown that when kernels satisfying (2) and (5) are properly scaled, so that $\mathcal{L}\to\Delta$, $\|\widehat{u}_n - \widehat{u}_l\|_{0,\Omega_l} \le C\varepsilon^2 + \mathcal{O}(\varepsilon^4)$. The same result holds for the peridynamics kernel in (58).

5 Approximation of the optimization-based LtN formulation

This section presents the discretization and the error analysis of the LtN formulation (14). Throughout this section we assume that η_c and Γ_c are polygonal domains; this assumption is not restrictive as those are virtual domains that we can define at our discretion.

5.1 Discretization

We use a reduced-space approach to solve the optimization-based LtN problem (14) numerically, i.e., we discretize and solve the problem

$$\min_{\theta_n,\theta_l} J(\theta_n,\theta_l) \quad \text{with} \quad J(\theta_n,\theta_l)\frac{1}{2}\|u_n(\theta_n)-u_l(\theta_l)\|^2_{0,\Omega_o} \tag{36}$$

where $u_n(\theta_n)\in V_{\eta_D}(\Omega_n)$ solves the weak nonlocal equation

$$B_n(u_n(\theta_n);z_n,\kappa_n) := \int\limits_{\Omega_n}\int\limits_{\Omega_n} \mathcal{G}u_n\cdot\mathcal{G}z_n\,d\boldsymbol{y}d\boldsymbol{x} + \int\limits_{\eta_c} u_n\kappa_n\,d\boldsymbol{x} = \int\limits_{\omega_n} f_n z_n\,d\boldsymbol{x} + \int\limits_{\eta_c}\theta_n\kappa_n\,d\boldsymbol{x}, \tag{37}$$

for all $(z_n,\kappa_n)\in V_{\eta_n}\times\Theta_n^*$, and $u_l(\theta_l)\in H^1_{\Gamma_D}(\Omega_l)$ solves the weak local equation

$$B_l(u_l(\theta_l);z_l,\kappa_l) := \int_{\Omega_l}\nabla u_l\nabla z_l\,d\boldsymbol{x} + \int_{\Gamma_c} u_l\kappa_l\,d\boldsymbol{x} = \int_{\Omega_l} f_l z_l\,d\boldsymbol{x} + \int_{\Gamma_c}\theta_l\kappa_l\,d\boldsymbol{x}, \tag{38}$$

for all $(z_l,\kappa_l)\in H^1_0(\Omega_l)\times\Theta_l^*$. Here, Θ_n^* and Θ_l^* are the duals of Θ_n and Θ_l, respectively.

To discretize (36)–(38) we consider the following conforming finite element spaces

$$\begin{aligned} &V^h_{\eta_D}\subset V_{\eta_D}(\Omega_n), \qquad \Theta^h_n\subset\Theta_n, \qquad V^h_{\eta_n}\times\Theta^h_n\subset V_{\eta_n}(\Omega_n)\times\Theta_n^*,\\ &H^h_{\Gamma_D}\subset H^1_{\Gamma_D}(\Omega_l), \qquad \Theta^h_l\subset\Theta_l, \qquad H^h_0\times\Theta^h_l\subset H^1_0(\Omega_l)\times\Theta_l^* \end{aligned} \tag{39}$$

for the nonlocal and local states, controls, and test functions[8], respectively. In general, the finite element spaces for the nonlocal and local problems can be defined on different meshes with parameters $h_n>0$ and $h_l>0$, respectively, and can have different polynomial orders given by integers $p_n\geq 1$ and $p_l\geq 1$, respectively.

Restriction of (36)–(38) to the finite element spaces (39) defines the discrete reduced-space LtN formulation

$$\min_{\theta^h_n,\theta^h_l} J_h(\theta^h_n,\theta^h_l) \quad \text{with} \quad J_h(\theta^h_n,\theta^h_l) = \frac{1}{2}\|u^h_n(\theta^h_n)-u^h_l(\theta^h_l)\|^2_{0,\Omega_o} \tag{40}$$

where $u^h_n(\theta^h_n)\in V^h_{\eta_D}$ solves the discrete nonlocal state equation

$$B_n(u^h_n(\theta^h_n);z^h_n,\kappa^h_n) = \int_{\omega_n} f_n z^h_n\,d\boldsymbol{x} + \int_{\eta_c}\theta^h_n\kappa^h_n\,d\boldsymbol{x}, \quad \forall\,(z^h_n,\kappa^h_n)\in V^h_{\eta_n}\times\Theta^h_n, \tag{41}$$

and $u^h_l(\theta^h_l)\in H^h_{\Gamma_D}$ solves the discrete local state equation[9]

$$B_l(u^h_l(\theta^h_l);z^h_l,\kappa^h_l) = \int_{\Omega_l} f_l z_l\,d\boldsymbol{x} + \int_{\Gamma_c}\theta^h_l\kappa^h_l\,d\boldsymbol{x}, \quad \forall\,(z^h_l,\kappa^h_l)\in H^h_0\times\Theta^h_l. \tag{42}$$

[8] For simplicity, we approximate Θ_n, Θ_l and their duals by the same finite dimensional space.
[9] Note that both (41) and (42) are well-posed.

Following Section 3.1, we write the solutions of (41) and (42) as

$$u_n^h = v_n^h + u_n^{h0} \quad \text{and} \quad u_l^h = v_l^h + u_l^{h0}, \tag{43}$$

where v_n^h and v_l^h are "harmonic" components solving (41) and (42) with $f_n = 0$ and $f_l = 0$ respectively, whereas u_n^{h0} and u_l^{h0} are "homogeneous" components solving (41) and (42) with $\theta_n^h = 0$ and $\theta_l^h = 0$, respectively. In terms of these components

$$J_h(\theta_n^h, \theta_l^h) = \frac{1}{2}\|v_n^h(\theta_n^h) - v_l^h(\theta_l^h)\|_{0,\Omega_o}^2 + \big(u_n^{h0} - u_l^{h0}, v_n^h(\theta_n^h) - v_l^h(\theta_l^h)\big)_{0,\Omega_o} + \frac{1}{2}\|u_n^{h0} - u_l^{h0}\|_{0,\Omega_o}^2 .$$

The Euler-Lagrange equation of (40) has the form: seek $(\sigma_n^h, \sigma_l^h) \in \Theta_n^h \times \Theta_l^h$ such that

$$Q_h(\sigma_n^h, \sigma_l^h; \mu_n^h, \mu_l^h) = F_h(\mu_n^h, \mu_l^h) \quad \forall\, (\mu_n^h, \mu_l^h) \in \Theta_n^h \times \Theta_l^h, \tag{44}$$

where $Q_h(\sigma_n^h, \sigma_l^h; \mu_n^h, \mu_l^h) = \big(v_n^h(\sigma_n^h) - v_l^h(\sigma_l^h),\, v_n^h(\mu_n^h) - v_l^h(\mu_l^h)\big)_{0,\Omega_o}$ and $F_h(\mu_n^h, \mu_l^h) = -\big(u_n^{h0} - u_l^{h0}, v_n^h(\mu_n^h) - v_l^h(\mu_l^h)\big)_{0,\Omega_o}$. To prove the positivity of Q_h, the arguments of Lemma 3.1 cannot be extended, as the identity principle does not hold for v_l^h. We use instead the discrete strong Cauchy-Schwarz inequality in Lemma A.4.

Lemma 5.1: The form $Q_h(\cdot, \cdot)$ defines an inner product on $\Theta_n^h \times \Theta_l^h$.

Proof. We prove that $Q_h(\sigma_n^h, \sigma_l^h; \sigma_n^h, \sigma_l^h) = 0$ if and only if $(\sigma_n^h, \sigma_l^h) = (0, 0)$. If $(\sigma_n^h, \sigma_l^h) = (0, 0)$ then $v_n^h(\sigma_n^h) = 0$ and $v_l^h(\sigma_l^h) = 0$, implying $Q_h(\sigma_n^h, \sigma_l^h; \sigma_n^h, \sigma_l^h) = 0$. Conversely, if $Q_h(\sigma_n^h, \sigma_l^h; \sigma_n^h, \sigma_l^h) = 0$, then

$$0 = Q_h(\sigma_n^h, \sigma_l^h; \sigma_n^h, \sigma_l^h) = \|v_n^h(\sigma_n^h)\|_{0,\Omega_o}^2 + \|v_l^h(\sigma_l^h)\|_{0,\Omega_o}^2 - 2(v_n^h(\sigma_n^h), v_l^h(\sigma_l^h))_{0,\Omega_o}.$$

The discrete strong Cauchy-Schwarz inequality (see Lemma A.4) then implies

$$0 \geq (1 - \delta)(\|v_n^h(\sigma_n^h)\|_{0,\Omega_o}^2 + \|v_l^h(\sigma_l^h)\|_{0,\Omega_o}^2). \tag{45}$$

Since $\delta < 1$ the left hand side in the above inequality is nonnegative. Thus, we must have that $v_n^h(\sigma_n^h) = 0$ and $v_l^h(\sigma_l^h) = 0$, which implies $(\sigma_n^h, \sigma_l^h) = (0, 0)$. □

Lemma A.5 proves that $\Theta_n^h \times \Theta_l^h$ is Hilbert with respect to the discrete energy norm

$$\|\mu_n^h, \mu_l^h\|_{h*}^2 := Q_h(\mu_n^h, \mu_l^h; \mu_n^h, \mu_l^h). \tag{46}$$

This fact, Lemma 5.1 and the projection theorem provide the following corollary.

Corollary 5.1: The reduced space problem (40) has a unique minimizer.

5.2 Convergence analysis

In this section we prove that the discrete solution $(\theta_n^{h*}, \theta_l^{h*})$ converges to the exact solution (θ_n^*, θ_l^*) assuming the latter belongs to the "raw" control space $\Theta_n \times \Theta_l$. This assumption mirrors the one made in [1] and is necessary because the continuous problem is well-posed in the completion of the raw control space. We prove this result under the following assumptions.

H.3 The optimal solution belongs to the raw space: $(\theta_n^*, \theta_l^*) \in \Theta_n \times \Theta_l$.

H.4 The kernel γ is translation invariant, i.e. $\gamma(\boldsymbol{x},\boldsymbol{y}) = \gamma(\boldsymbol{x}-\boldsymbol{y})$[10].

Let $(\theta_n^*, \theta_l^*) \in \Theta_n \times \Theta_l$ denote the optimal solution of (17) and $(\theta_n^{h*}, \theta_l^{h*}) \in \Theta_n^h \times \Theta_l^h$ be the optimal solution of its discretization (40). We denote the associated optimal states by (u_n^*, u_l^*), and (u_n^{h*}, u_l^{h*}), respectively, that is,

$$(u_n^*, u_l^*) = (u_n(\theta_n^*), u_l(\theta_l^*)) \quad \text{and} \quad (u_n^{h*}, u_l^{h*}) = (u_n^h(\theta_n^{h*}), u_l(\theta_l^{h*})).$$

We will estimate the discrete energy norm of the error $(\theta_n^* - \theta_n^{h*}; \theta_l^* - \theta_l^{h*})$ using Strang's second[11] Lemma; see, e.g., [18, Lemma 2.25, p.94]. Application of this lemma is contingent upon two conditions: (i) the discrete form Q_h is continuous and coercive with respect to $\|\cdot\|_{h*}$, and (ii) there exists a positive real constant C such that

$$\|\mu_n, \mu_l\|_{h*} \le C\|\mu_n, \mu_l\|_* \quad \forall\, (\mu_n, \mu_l) \in \Theta_n \times \Theta_l\,. \tag{47}$$

The first assumption holds trivially. To verify (47) note that

$$\|\mu_n, \mu_l\|_{h*}^2 := Q_h(\mu_n, \mu_l; \mu_n, \mu_l) = \|v_n^h(\mu_n) - v_l^h(\mu_l)\|_{0,\Omega_o}^2\,.$$

Given $\mu_l \in \Theta_l$ the function $v_l^h(\mu_l)$ solves the weak equation

$$B_l(v_l^h(\mu_l); z_l^h, \kappa_l^h) = \int_{\Gamma_c} \mu_l \kappa_l^h\, d\boldsymbol{x} = \int_{\Gamma_c} \Pi_l(\mu_l)\kappa_l^h\, d\boldsymbol{x} \quad \forall\, (z_l^h, \kappa_l^h) \in H_0^h \times \Theta_l^h,$$

where Π_l is the L^2 projection onto Θ_l^h, i.e., $v_l^h(\mu_l) = v_l^h(\Pi_l \mu_l)$. Similarly, we have that $v_n^h(\mu_n) = v_n^h(\Pi_n \mu_n)$, where Π_n is the L^2 projection onto Θ_n^h. Additionally, similarly to [1], we assume that there exist positive constants γ_n^*, γ_l^*, γ_{n*}, and γ_{l*} such that for h_n and h_l small enough the following inequalities hold:

$$\begin{aligned} \gamma_{n*}\|v_n(\sigma_n^h)\|_{0,\Omega_o} \le \|v_n^h(\sigma_n^h)\|_{0,\Omega_o} &\quad \le \gamma_n^*\|v_n(\sigma_n^h)\|_{0,\Omega_o} \\ \gamma_{l*}\|v_l(\sigma_l^h)\|_{0,\Omega_o} \le \|v_l^h(\sigma_l^h)\|_{0,\Omega_o} &\quad \le \gamma_l^*\|v_l(\sigma_l^h)\|_{0,\Omega_o}. \end{aligned} \tag{48}$$

The latter, the strong Cauchy-Schwarz inequality and the boundedness of the L^2 projection operators yield

$$\begin{aligned} \|\mu_n, \mu_l\|_{h*}^2 &= \|v_n^h(\mu_n) - v_l^h(\mu_l)\|_{0,\Omega_o}^2 = \|v_n^h(\Pi_n(\mu_n)) - v_l^h(\Pi_l(\mu_l))\|_{0,\Omega_o}^2 \\ &\le \|v_n^h(\Pi_n(\mu_n))\|_{0,\Omega_o}^2 + \|v_l^h(\Pi_l(\mu_l))\|_{0,\Omega_o}^2 \\ &\le \gamma_n^*\|v_n(\Pi_n(\mu_n))\|_{0,\Omega_o}^2 + \gamma_l^*\|v_l(\Pi_l(\mu_l))\|_{0,\Omega_o}^2 \\ &\le \frac{C_1}{1-\delta}\|v_n(\Pi_n(\mu_n)) - v_l(\Pi_l(\mu_l))\|_{0,\Omega_o}^2 \\ &= \frac{C_1}{1-\delta}\|\Pi_n\mu_n, \Pi_l\mu_l\|_*^2 \le \frac{C_2}{1-\delta}\|\mu_n, \mu_l\|_*^2. \end{aligned} \tag{49}$$

Application of Strang's second lemma then yields the following error estimate.

[10] Note that this assumption is not too restrictive; in fact, it is very common in nonlocal mechanics applications.
[11] The discrete problem (44) also fits in the setting of Strang's first Lemma [18, Lemma 2.27, p.95]. We use the second lemma because it simplifies the analysis.

Lemma 5.2: Let (θ_n^*, θ_l^*) and $(\theta_n^{h*}, \theta_l^{h*})$ be the solutions of (20) and (44), then

$$\begin{aligned}&\|(\theta_n^* - \theta_n^{h*}, \theta_l^* - \theta_l^{h*})\|_{h*} \leq \\ &\inf_{(\sigma_n^h,\sigma_l^h)} \|(\theta_n^* - \sigma_n^h, \theta_l^* - \sigma_l^h)\|_{h*} + \sup_{\|(\mu_n^h,\mu_l^h)\|_{h*}=1} |Q_h(\theta_n^*, \theta_l^*; \mu_n^h, \mu_l^h) - F_h(\mu_n^h, \mu_l^h)|\end{aligned} \tag{50}$$

where (σ_n^h, σ_l^h), $(\mu_n^h, \mu_l^h) \in \Theta_n^h \times \Theta_l^h$.

We use the result in Lemma 5.2 to obtain asymptotic convergence rates under the assumption that 1) the homogeneous problems (19) have solutions $u_n^0 \in H^{p_n+t}(\Omega_n)$, for $t \in [0,1]$, and $u_l^0 \in H^{p_l+1}(\Omega_l)$; 2) the control variables (θ_n, θ_l) are such that $u_n(\theta_n) \in H^{p_n+t}(\Omega_n)$ and $u_l(\theta_l) \in H^{p_l+1}(\Omega_l)$. We treat the first term in (50) by using the norm-equivalence (67); we have

$$\begin{aligned}\inf_{(\sigma_n^h,\sigma_l^h)} \|(\theta_n^* - \sigma_n^h, \theta_l^* - \sigma_l^h)\|_{h*}^2 &= \inf_{(\sigma_n^h,\sigma_l^h)} \|(\Pi_n\theta_n^* - \sigma_n^h, \Pi_l\theta_l^* - \sigma_l^h)\|_{h*}^2 \\ &\leq C \inf_{(\sigma_n^h,\sigma_l^h)} \|(\Pi_n\theta_n^* - \sigma_n^h, \Pi_l\theta_l^* - \sigma_l^h)\|_{\Theta_n\times\Theta_l}^2 = 0,\end{aligned} \tag{51}$$

where $\|\cdot\|_{\Theta_n\times\Theta_l}$ is defined as in (15). We focus on the second term in (50). Adding and subtracting $Q(\theta_n^*, \theta_l^*; \mu_n^h, \mu_l^h)$ and using conformity of $\Theta_n^h \times \Theta_l^h$ gives

$$\begin{aligned}&Q_h(\theta_n^*, \theta_l^*; \mu_n^h, \mu_l^h) - F_h(\mu_n^h, \mu_l^h) = \\ &\quad= \big[Q_h(\theta_n^*, \theta_l^*; \mu_n^h, \mu_l^h) - Q(\theta_n^*, \theta_l^*; \mu_n^h, \mu_l^h)\big] + \big[Q(\theta_n^*, \theta_l^*; \mu_n^h, \mu_l^h) - F_h(\mu_n^h, \mu_l^h)\big] \\ &\quad= \big[Q_h(\theta_n^*, \theta_l^*; \mu_n^h, \mu_l^h) - Q(\theta_n^*, \theta_l^*; \mu_n^h, \mu_l^h)\big] + \big[F(\mu_n^h, \mu_l^h) - F_h(\mu_n^h, \mu_l^h)\big].\end{aligned}$$

Adding and subtracting the terms

$$(v_n(\theta_n^*) - v_l(\theta_l^*), v_n^h(\mu_n^h) - v_l^h(\mu_l^h))_{0,\Omega_o} \quad \text{and} \quad (u_n^0 - u_l^0, v_n^h(\mu_n^h) - v_l^h(\mu_l^h))_{0,\Omega_o}$$

to the last expression and using the definitions of Q, F, Q_h and F_h yields the identity:

$$\begin{aligned}&Q_h(\theta_n^*, \theta_l^*; \mu_n^h, \mu_l^h) - F_h(\mu_n^h, \mu_l^h) = \\ &\quad= \big((v_n^h(\theta_n^*) - v_n(\theta_n^*)) - (v_l^h(\theta_l^*) - v_l(\theta_l^*)), v_n^h(\mu_n^h) - v_l^h(\mu_l^h)\big)_{0,\Omega_o} + \\ &\quad\big((u_n^{h0} - u_n^0) - (u_l^{h0} - u_l^0), v_n^h(\mu_n^h) - v_l^h(\mu_l^h)\big)_{0,\Omega_o} + \\ &\quad\big(u_n^* - u_l^*, (v_n^h(\mu_n^h) - v_n(\mu_n^h)) - (v_l^h(\mu_l^h) - v_l(\mu_l^h))\big)_{0,\Omega_o}.\end{aligned}$$

Application of the Cauchy-Schwartz inequality then gives the following upper bound:

$$\begin{aligned}&\big|Q_h(\theta_n^*, \theta_l^*; \mu_n^h, \mu_l^h) - F_h(\mu_n^h, \mu_l^h)\big| \leq \|v_n^h(\mu_n^h) - v_l^h(\mu_l^h)\|_{0,\Omega_o} \times \\ &\quad\Big(\|v_n^h(\theta_n^*) - v_n(\theta_n^*)\|_{0,\Omega_o} + \|v_l^h(\theta_l^*) - v_l(\theta_l^*)\|_{0,\Omega_o} + \|u_n^{h0} - u_n^0\|_{0,\Omega_o} + \|u_l^{h0} - u_l^0\|_{0,\Omega_o}\Big) + \\ &\quad\Big(\|v_n^h(\mu_n^h) - v_n(\mu_n^h)\|_{0,\Omega_o} + \|v_l^h(\mu_l^h) - v_l(\mu_l^h)\|_{0,\Omega_o}\Big) \times \|u_n^* - u_l^*\|_{0,\Omega_o}.\end{aligned}$$

Furthermore, note that $\|v_n^h(\mu_n^h) - v_l^h(\mu_l^h)\|_{0,\Omega_o} = \|\mu_n^h, \mu_l^h\|_{h*} = 1$, and that $\|u_n^* - u_l^*\|_{0,\Omega_o} = J(u_n^*, u_l^*)$ is the optimal value of the objective functional, which is bounded by the modeling error. The regularity assumptions on the nonlocal solutions in (19) allow us to apply Theorem 6.2 in [16, p.689]:

$$\|u_n^{h0} - u_n^0\|_{0,\Omega_o} \leq C\, h_n^{p_n+t} \|u_n^0\|_{p_n+t,\Omega_n},$$

where $t \in [0,1]$. Furthermore, the regularity assumptions on the local solutions in (19) allow us to use Corollary 1.122 in [18, p.66] to conclude that

$$\|u_l^{h0} - u_l^0\|_{0,\Omega_o} \leq C h_l^{p_l+1} \|u_l^0\|_{p_l+1,\Omega_l}.$$

According to Weyl's Lemma [31] the local harmonic liftings $v_l(\theta_l^*)$ and $v_l(\mu_l^h)$ are smooth functions and so there are positive constants C_1 and C_2 such that

$$\|v_l^h(\theta_l^*) - v_l(\theta_l^*)\|_{0,\Omega_o} \leq C_1 h_l^{p_l+1} \quad \text{and} \quad \|v_l^h(\mu_l^h) - v_l(\mu_l^h)\|_{0,\Omega_o} \leq C_2 h_l^{p_l+1}.$$

While a similar result holds for the nonlocal harmonic lifting $v_n(\theta_n^*)$, the treatment of $v_n(\mu_n^h)$ is more involved, due to the discrete nature of the Dirichlet data, and it requires an auxiliary function $\widetilde{\mu}_n \in C^\infty(\eta_c)$ such that $\|\widetilde{\mu}_n - \mu_n^h\|_{L^2(\eta_c)} \leq \epsilon$, for an arbitrarily small ϵ. Because v_n and v_n^h depend continuously on the data,

$$\begin{aligned}
&\|v_n^h(\mu_n^h) - v_n(\mu_n^h)\|_{0,\Omega_o} \\
&\leq \|v_n^h(\mu_n^h) - v_n^h(\widetilde{\mu}_n)\|_{0,\Omega_o} + \|v_n^h(\widetilde{\mu}_n) - v_n(\widetilde{\mu}_n)\|_{0,\Omega_o} + \|v_n(\widetilde{\mu}_n) - v_n(\mu_n^h)\|_{0,\Omega_o} \\
&\leq C_1 h_n^{p_n+t} \|v_n(\widetilde{\mu}_n)\|_{p_n+t,\Omega_n} + \|v_n^h(\mu_n^h - \widetilde{\mu}_n)\|_{0,\Omega_o} + \|v_n(\widetilde{\mu}_n - \mu_n^h)\|_{0,\Omega_o} \\
&\leq C_1 h_n^{p_n+t} \|v_n(\widetilde{\mu}_n)\|_{p_n+t,\Omega_n} + C_2 \|\mu_n^h - \widetilde{\mu}_n\|_{0,\eta_c} + C_3 \|\widetilde{\mu}_n - \mu_n^h\|_{0,\eta_c}.
\end{aligned} \tag{52}$$

Since ϵ can be arbitrarily small, the last two terms in (52) are negligible. To complete the estimate we only need a uniform bound on $\|v_n(\widetilde{\mu}_n)\|_{p_n+t,\Omega_n}$. To this end, assume that for all $\widetilde{\mu}_n \in C^\infty(\eta_c)$, $v_n(\widetilde{\mu}_n) \in C^k(\Omega_n)$ with $k = p_n + t$. Under this assumption $\mathrm{D}^\beta[\mathcal{L} v_n(\widetilde{\mu}_n)] = \mathcal{L}\mathrm{D}^\beta[v_n(\widetilde{\mu}_n)]$ for all $\beta \leq k$. Taking into account that $v_n(\widetilde{\mu}_n)$ is nonlocal harmonic, i.e., $\mathcal{L} v_n(\widetilde{\mu}_n) = 0$, it follows that $\mathcal{L}\mathrm{D}^\beta[v_n(\widetilde{\mu}_n)] = 0$, i.e., $\mathrm{D}^\beta[v_n(\widetilde{\mu}_n)]$ is also nonlocal harmonic for all $\beta \leq k$. Thus, $\mathrm{D}^\beta[v_n(\widetilde{\mu}_n)]$ has a uniformly bounded L^2 norm, i.e. $\|\mathrm{D}^\beta[v_n]\|_{0,\Omega_n} \leq C_\beta,\ \forall\, \beta \leq k$. This implies the existence of a positive constant C such that, $\|v_n(\widetilde{\mu}_n)\|_{p_n+t,\Omega_n} \leq C$. It follows that there exist positive constants C_1 and C_2 such that

$$\|v_n^h(\theta_n^*) - v_n(\theta_n^*)\|_{0,\Omega_o} \leq C_1 h_n^{p_n+t} \quad \text{and} \quad \|v_n^h(\mu_n^h) - v_n(\mu_n^h)\|_{0,\Omega_o} \leq C_2 h_n^{p_n+t}.$$

We have just shown the following result.

Theorem 5.1: Assume that H.1–H.4 hold. Then, there exist positive constants C_1, C_2 such that

$$\|(\theta_n^* - \theta_n^{h*}, \theta_l^* - \theta_l^{h*})\|_{h*} \leq C_1 h_n^{p_n+t} + C_2 h_l^{p_l+1}. \tag{53}$$

We use Theorem 5.1 to estimate the $\Theta_n \times \Theta_l$ norm of the discretization error.

Corollary 5.2: Assume that H.1–H.4 hold. Then, there exist positive constants C_1, C_2, C_3 such that

$$\|(\theta_n^* - \theta_n^{h*}, \theta_l^* - \theta_l^{h*})\|^2_{\Theta_n \times \Theta_l} \leq C_1 h_n^{2(p_n+t)} + C_2 h_l^{2p_l+1}. \tag{54}$$

Proof. Adding and subtracting $\Pi_n \theta_n^*$ and $\Pi_l \theta_l^*$, and using the triangle inequality

$$\begin{aligned}
&\|(\theta_n^* - \theta_n^{h*}, \theta_l^* - \theta_l^{h*})\|_{\Theta_n \times \Theta_l} \\
&\quad\leq \|(\theta_n^* - \Pi_n \theta_n^*, \theta_l^* - \Pi_l \theta_l^*)\|_{\Theta_n \times \Theta_l} + \|(\Pi_n \theta_n^* - \theta_n^{h*}, \Pi_l \theta_l^* - \theta_l^{h*})\|_{\Theta_n \times \Theta_l}.
\end{aligned} \tag{55}$$

Using standard finite element approximation results for the first term yields

$$\|(\theta_n^* - \Pi_n \theta_n^*, \theta_l^* - \Pi_l \theta_l^*)\|^2_{\Theta_n \times \Theta_l} \leq C_2 h_n^{2(p_n+t)} \|\theta_n^*\|^2_{p_n+t,\eta_c} + C_3 h_l^{2p_l+1} \|\theta_l^*\|^2_{p_l+\frac{1}{2},\Gamma_c}. \tag{56}$$

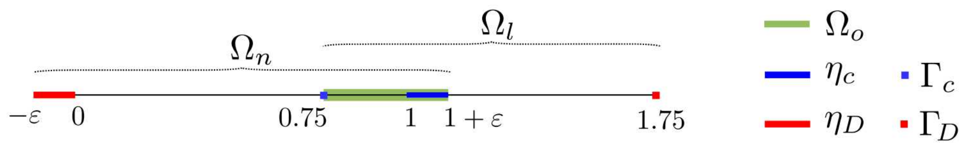

Fig. 3: One-dimensional LtN configuration used in the numerical tests.

We focus on the second term in (55). By the norm-equivalence (67) in the discrete control space, we have

$$\|(\Pi_n\theta_n^* - \theta_n^{h*}, \Pi_n\theta_n^* - \theta_l^{h*})\|_{\Theta_n\times\Theta_l} \leq C\|(\Pi_n\theta_n^* - \theta_n^{h*}, \Pi_n\theta_n^* - \theta_l^{h*})\|_{h*} = C\|(\theta_n^* - \theta_n^{h*}, \theta_n^* - \theta_l^{h*})\|_{h*}.$$

This result along with (53) and (56) implies (54). □

Since u_n^* and u_l^* depend continuously on the data, (54), Corollary 5.2 implies that

$$\begin{aligned} \|u_n^* - u_n^{*h}\|_{0,\Omega_n}^2 &\leq K_{n1}\, h_n^{2(p_n+t)} + K_{n2}\, h_l^{2p_l+1} \\ \|u_l^* - u_l^{*h}\|_{0,\Omega_l}^2 &\leq K_{l1}\, h_n^{2(p_n+t)} + K_{l2}\, h_l^{2p_l+1}, \end{aligned} \tag{57}$$

that is, the L^2 norm error of the state variables is of the same order as the $L^2 \times H^{\frac{1}{2}}$ norm error of the controls.

6 Numerical tests

We present numerical tests with the new LtN formulation in one dimension, including a patch test, a convergence study and approximation of discontinuous solutions. Though preliminary, these results show the effectiveness of the coupling method, illustrate the theoretical results, and provide the basis for realistic simulations. In our examples we use an integrable kernel, γ_i, satisfying assumptions (2) and (5) to illustrate theoretical results and a singular kernel, γ_s, often used in the literature as an approximation of a peridynamic model for nonlocal mechanics. These kernels are given by

$$\gamma_i(x,y) = \frac{3}{2\varepsilon^3}\chi_{(x-\varepsilon,x+\varepsilon)}(y) \quad \text{and} \quad \gamma_s(x,y) = \frac{1}{\varepsilon^2|x-y|}\chi_{(x-\varepsilon,x+\varepsilon)}(y), \tag{58}$$

respectively. Even though γ_s does not satisfy our theoretical assumptions[12], these numerical results demonstrate the effectiveness of the LtN coupling for realistic, practically important, nonlocal models. In all examples we consider the LtN problem configuration shown in Fig. 3, where $\Omega_n = (-\varepsilon, 1+\varepsilon)$, $\eta_D = (-\varepsilon, 0)$, $\eta_c = (1, 1+\varepsilon)$, $\Omega_l = (0.75, 1.75)$, $\Gamma_D = 1.75$, $\Gamma_c = 0.75$, and $\Omega_o = (0.75, 1+\varepsilon)$. In all numerical tests $V_{\eta_D}^h$, $V_{\eta_n}^h$, and Θ_n^h are discontinuous piecewise linear finite element spaces, while $H_{\Gamma_D}^h$ and H_0^h are C^0 piecewise linear finite elements. We use the same grid size h for the local and nonlocal finite element spaces. To solve the LtN optimization problem we apply the gradient based Quasi-Newton scheme BFGS [26].

[12] The energy space associated with γ_s is not equivalent to a Sobolev space, nevertheless it is a separable Hilbert space whose energy norm satisfies a nonlocal Poincaré inequality.

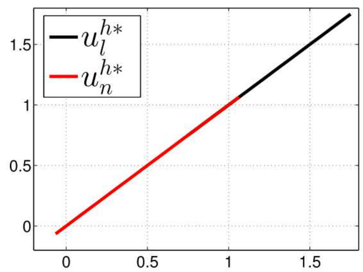

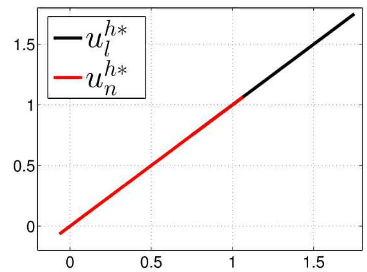

Fig. 4: Optimal states for the patch test with γ_i (left) and γ_s (right).

The patch test This test uses the linear manufactured solution $u_n = u_l = x$, $u_n|_{\eta_D} = x$, $u_l(1.75) = 1.75$, $f_n = f_l = 0$. We expect the LtN formulation to recover this solution exactly, i.e., $u_n^{h*} \equiv u_n^*$ and $u_n^{h*} \equiv u_l^*$. Figure 4 shows the optimal states u_n^{h*} and u_l^{h*}, computed with $\varepsilon = 0.065$ and $h = 2^{-7}$, for γ_i (left) and γ_s (right). The LtN method recovers the exact solution to machine precision.

Convergence tests We examine the convergence of finite element approximations with respect to the grid size h using the following manufactured solutions:

M.1 $u_n = u_l = x^2$, $u_n|_{\eta_D} = x^2$, $u_l(1.75) = 1.75^2$, $f_n = f_l = -2$.

M.2 $u_n = u_l = x^3$, $u_n|_{\eta_D} = x^3$, $u_l(1.75) = 1.75^3$, $f_n = f_l = -6x$.

Note that, for both kernels, the associated nonlocal operator is equavalent to the classical Laplacian for polynomials up to the third order. For examples **M.1** and **M.2** we compute the convergence rates and the L^2 norm of the errors for the nonlocal state, $e(u_n^*)$, the local state, $e(u_l^*)$, and the nonlocal control parameter, $e(\theta_n^*)$. The results are reported in Tables 1 and 2 for γ_i and in Tables 3 and 4 for γ_s in correspondence of different values of interaction radius ε and grid size h. In Fig. 5 we also report the optimal discrete solutions.

Results in Tables 1 and 2 show optimal convergence for state and control variables. We note that according to [16] and FE convergence theory [18] this is the same rate as for the independent discretization of the nonlocal and local equations by piecewise linear elements.

Remark 6.1: The convergence analysis in Section 5.2 establishes a suboptimal convergence rate in the L^2 norm of the discretization error of the state variables as we lose half order of convergence. We believe that the bound in (57) is not sharp, in fact, additional numerical tests (with $h = 2^{-8}, \ldots 2^{-12}$) show that there is no convergence deterioration.

For the singular kernel γ_s there are no theoretical convergence results; however, there is numerical evidence that piecewise linear approximations of (11) are second-order accurate; see [6]. Our numerical experiments in Tables 3 and 4 show that the optimization-based LtN solution converges at the same rate.

Recovery of singular features The tests in this section are motivated by nonlocal mechanics applications and demonstrate the effectiveness of the coupling method in the presence of point forces and discontinuities. We use the following two manufactured solution examples:

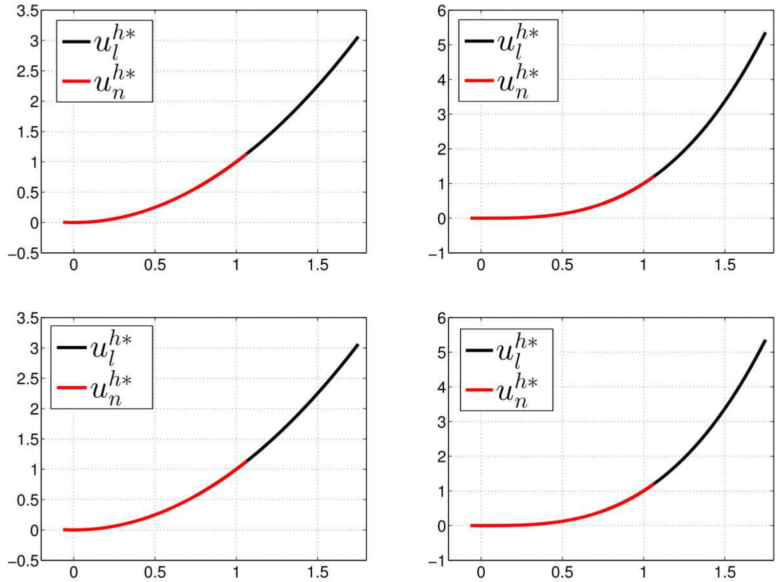

Fig. 5: Optimal states for **M.1** (left) and **M.2** (right) with γ_i (top) and γ_s (bottom).

ε	h	$e(u_n^*)$	rate	$e(u_l^*)$	rate	$e(\theta_n^*)$	rate
0.010	2^{-3}	2.63e-03	-	2.76e-03	-	5.59e-05	-
	2^{-4}	6.16e-04	2.10	6.74e-04	2.04	2.63e-05	1.09
	2^{-5}	1.40e-04	2.13	1.63e-04	2.05	1.14e-05	1.20
	2^{-6}	3.46e-05	2.02	4.04e-05	2.01	4.18e-06	1.47
	2^{-7}						
0.065	2^{-3}	2.24e-03	-	2.56e-03	-	6.34e-04	-
	2^{-4}	7.56e-04	1.56	7.13e-04	1.85	1.78e-04	1.83
	2^{-5}	1.89e-04	2.00	1.78e-04	2.00	4.46e-05	2.00
	2^{-6}	4.73e-05	2.00	4.46e-05	2.00	1.12e-05	2.00
	2^{-7}	1.18e-05	2.00	1.11e-05	2.00	2.82e-06	1.99

Tab. 1: Example **M.1** with γ_i: dependence on the grid size h and interaction radius ε of the error.

A.1 $u_n|_{\eta_D} = 0$, $u_l(1.75) = 0$, $f_n = f_l = \delta(x - 0.25)$, being δ the Dirac function.

A.2 $u_n|_{\eta_D} = 0$, $u_l(1.75) = 0$,

$$f_n = f_l = \begin{cases} 0 & x < \frac{1}{2} - \varepsilon \\ -\frac{2}{\varepsilon}\left(\frac{1}{2}\varepsilon^2 - \varepsilon + \frac{3}{8} + \left(2\varepsilon - \frac{3}{2} - \log\varepsilon\right)x + \right. \\ \qquad \left. \left(\frac{3}{2} + \log\varepsilon\right)x^2 - \log\left(\frac{1}{2} - x\right)(x^2 - x)\right) & \frac{1}{2} - \varepsilon \le x < \frac{1}{2} \\ -\frac{2}{\varepsilon}\left(\frac{1}{2}\varepsilon^2 - \varepsilon - \frac{3}{8} + \left(2\varepsilon + \frac{3}{2} + \log\varepsilon\right)x - \right. \\ \qquad \left. \left(\frac{3}{2} + \log\varepsilon\right)x^2 - \log\left(x - \frac{1}{2}\right)(x^2 - x)\right) & \frac{1}{2} \le x < \frac{1}{2} + \varepsilon \\ 0 & x \ge \frac{1}{2} + \varepsilon. \end{cases}$$

ε	h	$e(u_n^*)$	rate	$e(u_l^*)$	rate	$e(\theta_n^*)$	rate
0.010	2^{-3}	4.89e-03	-	1.09e-02	-	2.04e-04	-
	2^{-4}	1.23e-03	1.99	2.74e-03	2.00	9.63e-05	1.08
	2^{-5}	3.11e-04	1.99	6.86e-04	2.00	4.16e-05	1.21
	2^{-6}	7.85e-05	1.99	1.72e-04	2.00	1.45e-05	1.51
	2^{-7}	1.95e-05	2.01	4.29e-05	2.00	3.16e-06	2.20
0.065	2^{-3}	5.41e-03	-	1.09e-02	-	2.29e-03	-
	2^{-4}	1.34e-03	2.01	2.74e-03	2.00	5.46e-04	2.07
	2^{-5}	3.38e-04	1.99	6.86e-04	2.00	1.38e-04	1.99
	2^{-6}	8.46e-05	2.00	1.71e-04	2.00	3.46e-05	1.99
	2^{-7}	2.12e-05	2.00	4.29e-05	2.00	8.73e-06	1.99

Tab. 2: Example **M.2** with γ_i: dependence on the grid size h and interaction radius ε of the error.

ε	h	$e(u_n^*)$	rate	$e(u_l^*)$	rate	$e(\theta_n^*)$	rate
0.010	2^{-3}	2.67e-03	-	2.78e-03	-	5.79e-05	-
	2^{-4}	6.33e-04	2.08	6.81e-04	2.03	2.72e-05	1.09
	2^{-5}	1.47e-04	2.11	1.65e-04	2.04	1.19e-05	1.20
	2^{-6}	3.63e-05	2.01	4.11e-05	2.01	4.29e-06	1.47
	2^{-7}	9.10e-06	2.00	1.03e-05	2.00	1.05e-06	2.03
0.065	2^{-3}	2.36e-03	-	2.62e-03	-	6.52e-04	-
	2^{-4}	7.54e-04	1.65	7.12e-04	1.88	1.78e-04	1.87
	2^{-5}	1.88e-04	2.00	1.78e-04	2.00	4.45e-05	2.00
	2^{-6}	4.67e-05	2.01	4.44e-05	2.00	1.11e-05	2.00
	2^{-7}	1.14e-05	2.04	1.10e-05	2.01	2.76e-06	2.01

Tab. 3: Example **M.1** with γ_s: dependence on the grid size h and interaction radius ε of the error.

ε	h	$e(u_n^*)$	rate	$e(u_l^*)$	rate	$e(\theta_n^*)$	rate
0.010	2^{-3}	4.90e-03	-	1.09e-02	-	2.07e-04	-
	2^{-4}	1.23e-03	1.99	2.74e-03	2.00	9.68e-05	1.10
	2^{-5}	3.11e-04	1.99	6.86e-04	2.00	4.17e-05	1.21
	2^{-6}	7.85e-05	1.99	1.72e-04	2.00	1.46e-05	1.52
	2^{-7}	1.96e-05	2.01	4.29e-05	2.00	3.17e-06	2.00
0.065	2^{-3}	5.40e-03	-	1.09e-02	-	2.31e-03	-
	2^{-4}	1.34e-03	2.01	2.74e-03	2.00	5.46e-04	2.08
	2^{-5}	3.37e-04	1.99	6.86e-04	2.00	1.38e-04	2.00
	2^{-6}	8.46e-05	2.00	1.72e-04	2.00	3.46e-05	1.99
	2^{-7}	2.12e-05	2.00	4.29e-05	2.00	8.73e-06	1.99

Tab. 4: Example **M.2** with γ_s: dependence on the grid size h and interaction radius ε of the error.

In Fig. 6 we report the optimal discrete solutions for $h = 2^{-7}$ and $\varepsilon = 0.065$. In particular, **A.2** is a significant example that shows the usefulness of the coupling method in approximating the true solution with a local model where the nonlocality effects are not pronounced, i.e. the solution is smooth.

Acknowledgements

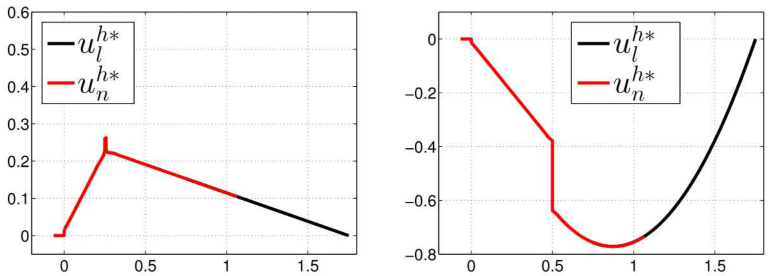

Fig. 6: Optimal states for examples **A.1** and **A.2**.

This material is based upon work supported by the U.S. Department of Energy, Office of Science, Office of Advanced Scientific Computing Research. Part of this research was carried under the auspices of the Collaboratory on Mathematics for Mesoscopic Modeling of Materials (CM4). This paper describes objective technical results and analysis. Any subjective views or opinions that might be expressed in the paper do not necessarily represent the views of the U.S. Department of Energy or the United States Government. SAND Number:

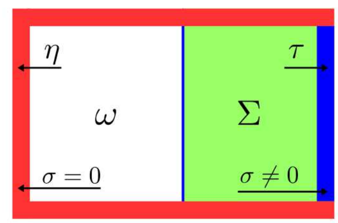

Fig. 7: Domain for Lemma A.1.

A Ancillary results

This appendix contains several results necessary for the well-posedness of the continuous and discrete reduced space problems and for the estimate of $\|H\|_{**}$. In the following results and proofs we let C and C_i, $i = 1, 2, \ldots$, be generic positive constants.

Lemma A.1: *[Nonlocal trace inequality]* Let $\Omega = \omega \cup \eta$ where ω and η are an open bounded domain and its associated interaction domain and let $\Sigma \subset \Omega$, $\tau \subset \eta$, $\tau \subset \Sigma$ as in Fig. 7. Assume that $\sigma \in \widetilde{V}(\eta)$ is such that $\sigma|_{\eta\setminus\tau} = 0$. Then

$$\|\sigma\|_{\widetilde{V}(\eta)} \leq C|||v|||_\Sigma \quad \forall\, v \in V(\Omega),\, v|_\eta = \sigma. \tag{59}$$

Proof. We need the following subspaces of $\widetilde{V}(\eta)$ and $V(\Omega)$

$$\begin{array}{ll} \widetilde{V}_{\eta\setminus\tau}(\eta) & = \{\mu \in \widetilde{V}(\eta),\ \mu|_{\eta\setminus\tau} = 0\} \ \subseteq \widetilde{V}(\eta), \\ V_{\eta\setminus\tau}(\Omega) & = \{w \in V(\Omega),\ w|_{\eta\setminus\tau} = 0\} \ \subseteq V(\Omega). \end{array} \tag{60}$$

Let χ_Σ be the indicator of Σ. Definition (4) and the fact that σ vanishes on $\eta \setminus \tau$ imply that

$$\|\sigma\|_{\widetilde{V}(\eta)} := \inf_{v\in V(\Omega),\, v|_\eta=\sigma} |||v|||_\Omega = \inf_{v\in V_{\eta\setminus\tau}(\Omega),\, v|_\eta=\sigma} |||v|||_\Omega \leq \inf_{v\in V_{\eta\setminus\tau}(\Omega),\, v|_\eta=\sigma} |||\chi_\Sigma v|||_\Omega.$$

To bound the energy norm of $\chi_\Sigma v$ note that

$$
\begin{aligned}
|||\chi_\Sigma v|||_\Omega^2 &= \int_\Omega\int_\Omega \big(\chi_\Sigma(\boldsymbol{x})v(\boldsymbol{x}) - \chi_\Sigma(\boldsymbol{y})v(\boldsymbol{y})\big)^2\gamma(\boldsymbol{x},\boldsymbol{y})\,d\boldsymbol{y}d\boldsymbol{x}\\
&= \int_\Sigma\int_\Sigma \big(v(\boldsymbol{x}) - v(\boldsymbol{y})\big)^2\gamma(\boldsymbol{x},\boldsymbol{y})\,d\boldsymbol{y}d\boldsymbol{x} + \int_{\Omega\setminus\Sigma}\int_\Sigma v(\boldsymbol{y})^2\gamma(\boldsymbol{x},\boldsymbol{y})\,d\boldsymbol{y}d\boldsymbol{x}\\
&+ \int_\Sigma\int_{\Omega\setminus\Sigma} v(\boldsymbol{x})^2\gamma(\boldsymbol{x},\boldsymbol{y})\,d\boldsymbol{y}d\boldsymbol{x}\\
&= |||v|||_\Sigma^2 + \int_\Sigma v(\boldsymbol{x})^2\int_{\Omega\setminus\Sigma}\gamma(\boldsymbol{x},\boldsymbol{y})\,d\boldsymbol{y}\,d\boldsymbol{x} + \int_\Sigma v(\boldsymbol{y})^2\int_{\Omega\setminus\Sigma}\gamma(\boldsymbol{x},\boldsymbol{y})\,d\boldsymbol{x}\,d\boldsymbol{y}\\
&\le |||v|||_\Sigma^2 + 2\gamma_1\|v\|_{0,\Sigma}^2 \le (1+2\gamma_1 C_{pn}^2)\,|||v|||_\Sigma^2,
\end{aligned}
$$

where the last two inequalities follow from (6) and (7) respectively. Thus,

$$
\|\sigma\|_{\widetilde{V}(\eta)} \le C \inf_{v\in V_{\eta\setminus\tau}(\Omega),\, v|_\eta=\sigma} |||v|||_\Sigma = C \inf_{v\in V(\Omega),\, v|_\eta=\sigma} |||v|||_\Sigma,
$$

with $C^2 = (1+2\gamma_1 C_{pn}^2)$. □

Lemma A.2: Let Ω, ω and η be defined as in Lemma A.1. The trace space $\widetilde{V}_{\eta\setminus\tau}(\eta)$ is a closed subspace of $L^2(\eta)$. Furthermore, for all $\mu\in\widetilde{V}_{\eta\setminus\tau}(\eta)$ we have that

$$
\|\mu\|_{\widetilde{V}(\eta)} \le C\|\mu\|_{0,\eta}. \tag{61}
$$

Proof. Consider a sequence $\{\mu^k\}\subset\widetilde{V}_{\eta\setminus\tau}(\eta)$ such that $\mu^k\to\mu^*$ in $L^2(\eta)$. To show that $\mu^*\in\widetilde{V}_{\eta\setminus\tau}(\eta)$ consider the function $v^*\in L^2(\Omega)$ such that $v^*|_\eta=\mu^*$ and $v^*|_\omega = 0$. To complete the proof it remains to show that v^* has finite energy norm. Using the norm equivalence in Lemma 2.1

$$
|||v^*|||_\Omega \le C^*\|v^*\|_{0,\Omega} = C^*\|\mu^*\|_{0,\eta} < \infty.
$$

Therefore, $v^*\in V(\Omega)$ and $v^*|_\eta = \mu^*$, hence $\mu^*\in\widetilde{V}_{\eta\setminus\tau}(\eta)$. Finally, let $w\in V(\Omega)$ be such that $w|_\eta=\mu$; by Lemmas A.1 and 2.1, $\|\mu\|_{\widetilde{V}(\eta)}\le C_1|||w|||_\eta \le C_2\|\mu\|_{0,\eta}$. □

Application of Lemma A.2 with $\eta=\eta_n$ and $\tau=\eta_c$ implies that the trace space $\widetilde{V}_{\eta_D}(\eta_n)$ is a closed subspace of $L^2(\eta_n)$, and thus it is a Hilbert space in the L^2 topology. We use this result to prove a strong Cauchy-Schwartz inequality for the nonlocal and local harmonic components of the states, i.e., the solutions to (18). This inequality is essential for the estimate of $\|H\|_{**}$.

Lemma A.3: There exists $\delta<1$ such that for all $(\sigma_n,\sigma_l)\in\Theta_n\times\Theta_l$

$$
|(v_n(\sigma_n), v_l(\sigma_l))_{0,\Omega_o}| < \delta\|v_n(\sigma_n)\|_{0,\Omega_o}\,\|v_l(\sigma_l)\|_{0,\Omega_o}. \tag{62}
$$

Proof. We prove (62) by contradiction. If (62) does not hold then for all $0<\epsilon<1$, there exist $(\sigma_n^\epsilon,\sigma_l^\epsilon)\in\Theta_n\times\Theta_l$ such that the corresponding harmonic components $v_n(\sigma_n^\epsilon)=v_n^\epsilon$ and $v_l(\sigma_l^\epsilon)$ satisfy $\|v_n^\epsilon\|_{0,\Omega_o}=1$ and $\|v_l^\epsilon\|_{0,\Omega_o}=1$ and

$$
(v_n(\sigma_n^\epsilon), v_l(\sigma_l^\epsilon))_{0,\Omega_o} \ge (1-\epsilon)\|v_n(\sigma_n^\epsilon)\|_{0,\Omega_o}\,\|v_l(\sigma_l^\epsilon)\|_{0,\Omega_o}. \tag{63}
$$

Note that

$$(1-\epsilon)\|v_n(\sigma_n^\epsilon)\|_{0,\Omega_o}\,\|v_l(\sigma_l^\epsilon)\|_{0,\Omega_o} \le (v_n(\sigma_n^\epsilon), v_l(\sigma_l^\epsilon))_{0,\Omega_o} \le \|v_n(\sigma_n^\epsilon)\|_{0,\Omega_o}\,\|v_l(\sigma_l^\epsilon)\|_{0,\Omega_o}.$$

This implies that the sequence of inner products converges, i.e. $(v_n^\epsilon, v_l^\epsilon)_{0,\Omega_o} \to 1$. Furthermore, since $\{v_n^\epsilon\}$ and $\{v_l^\epsilon\}$ are bounded, there exist subsequences, still denoted by $\{v_n^\epsilon\}$ and $\{v_l^\epsilon\}$, such that

$$v_n^\epsilon \rightharpoonup v_n^* \quad \text{in } L^2 \quad \text{and} \quad v_l^\epsilon \rightharpoonup v_l^* \quad \text{in } H^1. \tag{64}$$

Since H^1 is compactly embedded in L^2, we also have

$$v_l^\epsilon \to v_l^* \quad \text{in } L^2. \tag{65}$$

The weak convergence of the sequences also implies that $\|v_n^*\|_{0,\Omega_o} \le 1$ and $\|v_l^*\|_{0,\Omega_o} \le 1$. Properties (64) and (65) then imply that

$$\begin{aligned}
\lim_{\epsilon\to 1}(v_n^\epsilon, v_l^\epsilon)_{0,\Omega_o} &= \lim_{\epsilon\to 1}(v_n^\epsilon - v_n^*, v_l^\epsilon)_{0,\Omega_o} + \lim_{\epsilon\to 1}(v_n^*, v_l^\epsilon)_{0,\Omega_o} \\
&= \lim_{\epsilon\to 1}(v_n^\epsilon - v_n^*, v_l^*)_{0,\Omega_o} + \lim_{\epsilon\to 1}(v_n^\epsilon - v_n^*, v_l^\epsilon - v_l^*)_{0,\Omega_o} + (v_n^*, v_l^*)_{0,\Omega_o} \\
&= \lim_{\epsilon\to 1}(v_n^\epsilon, v_l^\epsilon - v_l^*)_{0,\Omega_o} - \lim_{\epsilon\to 1}(v_n^*, v_l^\epsilon - v_l^*)_{0,\Omega_o} + (v_n^*, v_l^*)_{0,\Omega_o} \\
&= (v_n^*, v_l^*)_{0,\Omega_o},
\end{aligned}$$

where the last inequality follows from the strong convergence of the local component:

$$(v_n^\epsilon, v_l^\epsilon - v_l^*)_{0,\Omega_o} \le \|v_n^\epsilon\|_{0,\Omega_o}\|v_l^\epsilon - v_l^*\|_{0,\Omega_o} = \|v_l^\epsilon - v_l^*\|_{0,\Omega_o} \to 0 \;\text{ as }\; \epsilon \to 1.$$

Thus,

$$1 = \lim_{\epsilon\to 1}(v_n^\epsilon, v_l^\epsilon)_{0,\Omega_o} = (v_n^*, v_l^*)_{0,\Omega_o} \le \|v_n^*\|_{0,\Omega_o}\|v_l^*\|_{0,\Omega_o} \le 1.$$

This means that $(v_n^*, v_l^*)_{0,\Omega_o} = \|v_n^*\|_{0,\Omega_o}\|v_l^*\|_{0,\Omega_o}$. This identity holds if and only if $v_l^* = \alpha v_n^*$ for some real α. To complete the proof we apply the same argument as in Lemma 3.1. On the one hand $v_n^* = 0$ in η_D and so, $v_l^* = 0$ in $\Omega_o \cap \eta_D$. On the other hand, v_l^* is harmonic in Ω_o and the identity principle implies that $v_l^* \equiv 0$ in Ω_o. Thus, (63) holds if and only if $v_n^* = v_l^* = 0$ in Ω_o, a contradiction. □

Lemma A.4: Let δ be the constant in Lemma A.3 and let v_n^h and v_l^h be the discrete harmonic components of the discrete state variables as in (43). Then, there exist $\overline{h}_n$ and $\overline{h}_l$ such that

$$|(v_n^h, v_l^h)_{0,\Omega_o}| < \delta\|v_n^h\|_{0,\Omega_o}\,\|v_l^h\|_{0,\Omega_o}, \quad \forall\; h_n \le \overline{h}_n,\; h_l \le \overline{h}_l. \tag{66}$$

Proof. In this proof we follow the same arguments of Lemma A.7 of [1].

Let $\{h_{nk}, h_{lk}\}_{k\ge 1}$ be a sequence of mesh sizes for the nonlocal and local finite element approximations such that $\{h_{nk}, h_{lk}\} \to 0$ as $k \to \infty$. Also, let v_n^{hk} and v_l^{hk} be the nonlocal and local discrete harmonic components corresponding to h_{nk} and h_{lk}. It is well-known [18] that the local finite element solution converges strongly in L^2 to the infinite-dimensional solution v_l as $k \to \infty$. Furthermore, paper [16] shows that when γ is such that (5) holds the nonlocal finite element solution converges strongly in the energy norm to the infinite-dimensional solution v_n. Due to the Poincaré inequality such convergence implies the storng convergence in the L^2 norm. Thus, we have

$$\lim_{k\to\infty} \|v_n - v_n^{hk}\|_{0,\Omega_o} = 0$$
$$\lim_{k\to\infty} \|v_l - v_l^{hk}\|_{0,\Omega_o} = 0.$$

Since the strong convergence in L^2 implies the weak convergence and the convergence in norm, the following are also true

$$\begin{aligned}\lim_{k\to\infty} (v_n^{hk}, v_l^{hk})_{0,\Omega_o} &= \quad (v_n, v_l)_{0,\Omega_o}\\ \lim_{k\to\infty} \|v_n^{hk}\|_{0,\Omega_o} &= \quad \|v_n\|_{0,\Omega_o}\\ \lim_{k\to\infty} \|v_l^{hk}\|_{0,\Omega_o} &= \quad \|v_l\|_{0,\Omega_o}.\end{aligned}$$

Using the strong Cauchy-Schwarz inequality (62), we obtain

$$\lim_{k\to\infty} \left|(v_n^{hk}, v_l^{hk})_{0,\Omega_o}\right| = |(v_n, v_l)_{0,\Omega_o}| \leq \delta\, \|v_n\|_{0,\Omega_o} \|v_l\|_{0,\Omega_o} = \delta \lim_{k\to\infty} \|v_n^{hk}\|_{0,\Omega_o} \|v_l^{hk}\|_{0,\Omega_o}.$$

Thus, $\exists\, \overline{\varepsilon} > 0$ such that $\forall\, \varepsilon \leq \overline{\varepsilon}$, $\exists\, \overline{h}_n,\, \overline{h}_l$ such that $\forall\, h_n \leq \overline{h}_n,\ h_l \leq \overline{h}_l$

$$\left|(v_n^{hk}, v_l^{hk})_{0,\Omega_o}\right| \leq \delta\, \|v_n^{hk}\|_{0,\Omega_o} \|v_l^{hk}\|_{0,\Omega_o}.$$

□

Lemma A.5: The space $\Theta_n^h \times \Theta_l^h$ is Hilbert with respect to the inner product $Q_h(\sigma_n^h, \sigma_l^h; \mu_n^h, \mu_l^h) = (v_n^h(\sigma_n^h) - v_l^h(\sigma_l^h), v_n^h(\mu_n^h) - v_l^h(\mu_l^h))_{0,\Omega_o}$.

Proof. By assumption $\Theta_n^h \times \Theta_l^h$ is a closed subspace $\Theta_n \times \Theta_l$. Thus, it is Hilbert with respect to $\|(\sigma_n^h, \sigma_l^h)\|_{\Theta_n\times\Theta_l}$. Let $\|(\sigma_n^h, \sigma_l^h)\|_{h*} = Q_h(\sigma_n^h, \sigma_l^h; \sigma_n^h, \sigma_l^h)$; we show that $\|(\sigma_n^h, \sigma_l^h)\|_{\Theta_n\times\Theta_l}$ and $\|(\sigma_n^h, \sigma_l^h)\|_{h*}$ are equivalent, i.e. there exist K_* and K^* such that

$$K_* \|(\sigma_n^h, \sigma_l^h)\|_{\Theta_n\times\Theta_l} \leq \|(\sigma_n^h, \sigma_l^h)\|_{h*} \leq K^* \|(\sigma_n^h, \sigma_l^h)\|_{\Theta_n\times\Theta_l}. \tag{67}$$

Using the well-posedness of the discrete problems, we have

$$\begin{aligned}\|(\sigma_n^h, \sigma_l^h)\|_{h*}^2 &= \|v_n^h(\sigma_n^h) - v_l^h(\sigma_l^h)\|_{0,\Omega_o}^2 \leq \|v_n^h(\sigma_n^h)\|_{0,\Omega_o}^2 + \|v_l^h(\sigma_l^h)\|_{0,\Omega_o}^2\\ &\leq C_1 \left(\|\sigma_n^h\|_{0,\eta_c}^2 + \|\sigma_l^h\|_{\frac12,\Gamma_c}^2\right).\end{aligned}$$

On the other hand, we have

$$\begin{aligned}\|\sigma_n^h\|_{0,\eta_c}^2 + \|\sigma_l^h\|_{\frac12,\Gamma_c}^2 &\leq \|v_n^h(\sigma_n^h)\|_{0,\Omega_o}^2 + C_2 \|v_l^h(\sigma_l^h)\|_{1,\Omega_o}^2 && \text{Local trace inequality}\\ &\leq \|v_n^h(\sigma_n^h)\|_{0,\Omega_o}^2 + C_3 \|v_l^h(\sigma_l^h)\|_{0,\Omega_o}^2 && \text{Local inverse inequality [7]}\\ &\leq C_4 \left(\|v_n^h(\sigma_n^h)\|_{0,\Omega_o}^2 + \|v_l^h(\sigma_l^h)\|_{0,\Omega_o}^2\right)\\ &\leq \frac{C_4}{1-\delta} \|v_n^h(\sigma_n^h) - v_l^h(\sigma_l^h)\|_{0,\Omega_o}^2 && \text{Strong Cauchy-Schwarz}\\ &= \frac{C_4}{1-\delta} \|(\sigma_n^h, \sigma_l^h)\|_{h*}^2.\end{aligned}$$

Choosing $K_* = \frac{1-\delta}{C_4}$ and $K^* = C_1$, we obtain (67). □

B Notation summary

In this appendix we report a summary of the notation we use for local and nonlocal domains. In Table 5 we report local entities on the left and nonlocal entities on the right (see Fig. 2 for a two-dimensional configuration).

Symbol	Definition	Symbol	Definition
Ω	$\omega \cup \eta$	ω	interior of Ω
Γ	$\partial\Omega$	η	interaction domain of ω
Ω_l	local subdomain	Ω_n	nonlocal subdomain, $\omega_n \cup \eta_n$
		ω_n	interior of Ω_n
Γ_l	$\partial\Omega_l$	η_n	interaction domain of ω_n
Γ_D	$\Gamma \cap \Gamma_l$	η_D	$\eta \cap \eta_n$
Γ_c	$\Gamma_l \setminus \Gamma_D$	η_c	$\eta_n \setminus \eta_D$
Ω_o	overlap domain, $\Omega_n \cap \Omega_l$		

Tab. 5: Symbols used to denote local (on the left) and nonlocal (on the right) entities.

References

[1] A. Abdulle, O. Jecker, and A. Shapeev. An optimization based coupling method for multiscale problems. Technical Report 36.2015, EPFL, Mathematics Institute of Computational Science and Engineering, Lausanne, Switzerland, December 2015.

[2] B. Aksoylu and T. Mengesha. Results on nonlocal boundary value problems. *Numerical Functional Analysis and Optimization*, 31(12):1301–1317, 2010.

[3] B. Aksoylu and M. L. Parks. Variational theory and domain decomposition for nonlocal problems. *Applied Mathematics and Computation*, 217(14):6498 – 6515, 2011.

[4] F. Andreu-Vaillo, J.M. Mazón, J.D. Rossi, and J.J. Toledo-Melero. *Nonlocal diffusion problems*. American Mathematical Society ; Real Sociedad Matemática Española, 2010.

[5] Y. Azdoud, F. Han, and G. Lubineau. A morphing framework to couple non-local and local anisotropic continua. *International Journal of Solids and Structures*, 50(9):1332 – 1341, 2013.

[6] X. Chen and M. D. Gunzburger. Continuous and discontinuous finite element methods for a peridynamics model of mechanics. *Computer Methods in Applied Mechanics and Engineering*, 200(9–12):1237 – 1250, 2011.

[7] P. Ciarlet. *The Finite Element Method for Elliptic Problems*. SIAM Classics in Applied Mathematics. SIAM, Philadelphia, 2002.

[8] M. D'Elia and P. Bochev. Optimization-based coupling of nonlocal and local diffusion models. In R. Lipton, editor, *Proceedings of the Fall 2014 Materials Research Society Meeting*, MRS Symposium Proceedings, Boston, MA, November 2014. Cambridge University Press.

[9] M. D'Elia, Q. Du, M. D. Gunzburger, and R. B. Lehoucq. Finite range jump processes and volume–constrained diffusion problems. *Computational Methods in Applied Mathematics*, (29), 2017.

[10] M. D'Elia, M. Perego, P. Bochev, and D. Littlewood. A coupling strategy for nonlocal and local diffusion models with mixed volume constraints and boundary conditions. *Computers & Mathematics with Applications*, 71(11):2218 – 2230, 2016. Proceedings of the conference on Advances in Scientific Computing and Applied Mathematics. A special issue in honor of Max Gunzburger's 70th birthday.

[11] H. B. Dhia and G. Rateau. The Arlequin method as a flexible engineering design tool. *International Journal for Numerical Methods in Engineering*, 62(11):1442–1462, 2005.

[12] M. Di Paola, G. Failla, and M. Zingales. Physically-based approach to the mechanics of strong non-local linear elasticity theory. *Journal of Elasticity*, 97(2):103–130, 2009.

[13] M. Discacciati, P. Gervasio, and A. Quarteroni. The interface control domain decomposition (icdd) method for elliptic problems. *SIAM Journal on Control and Optimization*, 51(5):3434–3458, 2013.

[14] Q. Du. Optimization based nonoverlapping domain decomposition algorithms and their convergence. *SIAM Journal on Numerical Analysis*, 39(3):1056–1077, 2001.

[15] Q. Du and M. D. Gunzburger. A gradient method approach to optimization-based multidisciplinary simulations and nonoverlapping domain decomposition algorithms. *SIAM Journal on Numerical Analysis*, 37(5):pp. 1513–1541, 2000.

[16] Q. Du, M. D. Gunzburger, R. B. Lehoucq, and K. Zhou. Analysis and approximation of nonlocal diffusion problems with volume constraints. *SIAM Review*, 54(4):667–696, 2012.

[17] Q. Du, M. D. Gunzburger, R. B. Lehoucq, and K. Zhou. A nonlocal vector calculus, nonlocal volume-constrained problems and nonlocal balance lows. *Mathematical Models and Methods in Applied Sciences*, 23(03):493–540, 2013.

[18] A. Ern and J.-L. Guermond. *Theory and Practice of Finite Elements*. Number 159 in Applied Mathematical Sciences. Springer Verlag, New York, 2004.

[19] P. Gervasio, J.-L. Lions, and A. Quarteroni. Heterogeneous coupling by virtual control methods. *Numerische Mathematik*, 90:241–264, 2001. 10.1007/s002110100303.

[20] M. D. Gunzburger, M. Heinkenschloss, and H. K. Lee. Solution of elliptic partial differential equations by an optimization-based domain decomposition method. *Applied Mathematics and Computation*, 113(2-3):111 – 139, 2000.

[21] M. D. Gunzburger and H. K. Lee. An optimization-based domain decomposition method for the Navier-Stokes equations. *SIAM Journal on Numerical Analysis*, 37(5):pp. 1455–1480, 2000.

[22] M. D. Gunzburger, J. S. Peterson, and H. Kwon. An optimization based domain decomposition method for partial differential equations. *Computers & Mathematics with Applications*, 37(10):77 – 93, 1999.

[23] F. Han and G. Lubineau. Coupling of nonlocal and local continuum models by the Arlequin approach. *International Journal for Numerical Methods in Engineering*, 89(6):671–685, 2012.

[24] P. Kuberry and H. Lee. A decoupling algorithm for fluid-structure interaction problems based on optimization. *Computer Methods in Applied Mechanics and Engineering*, 2013.

[25] G. Lubineau, Y. Azdoud, F. Han, C. Rey, and A. Askari. A morphing strategy to couple non-local to local continuum mechanics. *Journal of the Mechanics and Physics of Solids*, 60(6):1088 – 1102, 2012.

[26] J. Nocedal and S. Wright. *Numerical Optimization*. Springer Verlag, New York, 1999.

[27] D. Olson, P. Bochev, M. Luskin, and A. Shapeev. An optimization-based atomistic-to-continuum coupling method. *SIAM Journal on Numerical Analysis*, 52(4):2183–2204, 2014.

[28] D. Olson, P. Bochev, M. Luskin, and A. V. Shapeev. Development of an optimization-based atomistic-to-continuum coupling method. In Ivan Lirkov, Svetozar Margenov, and Jerzy Waśniewski, editors, *Large-Scale Scientific Computing*, volume 8353 of *Lecture Notes in Computer Science*, pages 33–44. Springer Berlin Heidelberg, 2014.

[29] P. Seleson, S. Beneddine, and S. Prudhomme. A force-based coupling scheme for peridynamics and classical elasticity. *Computational Materials Science*, 66:34–49, 2013.

[30] S. A. Silling and R. B. Lehoucq. Peridynamic theory of solid mechanics. volume 44 of *Advances in Applied Mechanics*, pages 73 – 168. Elsevier, 2010.

[31] H. Weyl. The method of orthogonal projection in potential theory. *Duke Math. J.*, 7(1):411–444, 1940.